

ความผิดปกติของแอมพลิจูดในข้อมูลคลื่นไหวสะเทือนจากการวิเคราะห์ด้วยวิธี
ROCK PHYSICS และ AVO บริเวณแหล่งสิริกิติ์ แอ่งพิษณุโลก
จังหวัดกำแพงเพชร

ภัพธนันท์ ภัคสุขนิธิวัฒน์

งานนี้เป็นส่วนหนึ่งของการศึกษาตามหลักสูตรปริญญาวิทยาศาสตรบัณฑิต
ภาควิชาธรณีวิทยา คณะวิทยาศาสตร์
จุฬาลงกรณ์มหาวิทยาลัย ปีการศึกษา 2554
ลิขสิทธิ์ของจุฬาลงกรณ์มหาวิทยาลัย

SEISMIC AMPLITUDE ANOMALIES BY USING ROCK
PHYSICS AND AVO IN SIRIKIT FIELD AREA,
PITSANULOK BASIN, CHANGWAT KAMPHAENGPHEET

Miss Phatthanun Phaksuknithiwat

A Report Submitted in Partial Fulfillment of the Requirements for the
Bachelor of Science, Department of Geology,
Chulalongkorn University, 2011

...../...../.....

Date of submit

...../...../.....

Date of Approval

.....

(Dr. ThanopThitimakorn)

Senior Project Advisor

ชื่อโครงการวิจัย	ความผิดปกติของแอมพลิจูดในข้อมูลคลื่นไหวสะเทือนจากการวิเคราะห์ด้วยวิธี Rock physics และ AVO บริเวณแหล่งสิริกิติ์ แอ่งพิษณุโลก จังหวัดกำแพงเพชร
นิสิตผู้เสนอโครงการ	ภัทธนันท์ ภัคศุขนิธิวัฒน์ รหัสนิสิต 5132719423
อาจารย์ที่ปรึกษา	อ.ดร.ฐานบ ธิติมากร
ภาควิชา	ธรณีวิทยา คณะวิทยาศาสตร์ จุฬาลงกรณ์มหาวิทยาลัย
ปีการศึกษา	2554

บทคัดย่อ

ความผิดปกติของแอมพลิจูดในข้อมูลคลื่นไหวสะเทือนเป็นเครื่องมือที่สำคัญที่ใช้บ่งบอกไฮโดรคาร์บอน แต่อย่างไรก็ตามความผิดปกติดังกล่าวนี้สามารถเกิดได้จากหลายสาเหตุ ดังนั้นการหาสาเหตุการเกิดและจำแนกรูปแบบเอวีโอจึงเป็นจุดประสงค์ในการศึกษา ในการศึกษาครั้งนี้ข้อมูลที่ใช้มาจากแหล่งสิริกิติ์ ในแอ่งสะสมตะกอนพิษณุโลก

เทคนิคที่ใช้ในการศึกษานี้คือ Rock physics และ เอวีโอ ขั้นตอนแรกเริ่มจากการพล็อตค่าคุณสมบัติของหิน จากนั้นทำการจำลองคุณสมบัติของหินจากการแทนที่โดย น้ำ 100% น้ำมัน 80% และแก๊ส 80% เพื่อสังเกตการเปลี่ยนแปลงของค่า Acoustic impedance ในของเหลวแต่ละชนิด โดยจากการจำลองนี้ ค่าแนวโน้มการเปลี่ยนแปลง Acoustic impedance จะใช้ในการแบ่งแยกประเภทของเอวีโอสุดท้าย Synthetic AVO gathers ถูกสร้างเพื่อสังเกตการตอบสนองของแอมพลิจูดในข้อมูลคลื่นไหวสะเทือนในแต่ละชนิดของของเหลว ชุดหินทรายที่สนใจในพื้นที่ศึกษานี้ คือ ที่ความลึก 868-878 เมตร และ ความลึก 1252-1402 เมตร

จากผลการศึกษาพบว่า เมื่อพิจารณารอยต่อของหินดินดานปิดทับหินทราย ชั้นทรายทั้งสอง ความลึกมีค่า Acoustic impedance น้อยกว่าหินดินดานที่ปิดทับซึ่งจัดเป็น เอวีโอ ประเภทที่สอง และสาม ตามการระบบการจัดแบ่งประเภทของ Rutherford ในส่วนการจำลองเอวีโอพบว่าชั้นหินที่สนใจทั้งสองความลึกมีค่า Intercept – gradient ลดลงเมื่อมุมเพิ่มขึ้น และค่า Reflection coefficient เป็นลบ ซึ่งก็สอดคล้องกับการวิเคราะห์ในขั้นต้น และลักษณะธรณีวิทยาของพื้นที่นี้ แต่อย่างไรก็ตามการจำลองดังกล่าวยังมีข้อจำกัดในเรื่องความหนา ถ้าหากความหนาของชั้นหินที่สนใจน้อยกว่าค่า tuning thicknesses โดยเฉพาะที่ชั้นลึก

Title	SEISMIC AMPLITUDE ANOMALIES BY USING ROCK PHYSICS AND AVO IN SIRIKIT FIELD AREA, PITSANULOK BASIN, CHANGWAT KAMPHAENGPHEE
Researcher	Phatthanun Phaksuknithiwat ID 5132719423
Advisor	Dr. Thanop Thitinakorn
Department	Geology, Faculty of Science, Chulalongkorn University
Academic year	2011

Abstract

Seismic amplitude anomalies are the significant tools as a hydrocarbon-indicator; however, these anomalies can be originated by many causes. To investigate the causes of anomalies and classify their AVO (Amplitude-Versus-Offset) classes are the aim of this research. In this study the data from Sirikit petroleum field in Pitsanulok Basin were used.

The techniques used in this study are Rock physics and AVO modeling. Firstly the several cross-plots of petrophysical parameters were performed. Then, fluids-substitution was modeled with 100% of water and 80% of gas and oil to observe the variations of impedances with particular fluids. Based on the models, acoustic impedance trends were used to classify classes of AVO responses. Lastly, Synthetic AVO gathers were generated in order to observe the seismic amplitudes with different types of fluids. The interested sand formations in this study area are 868-878 meters and 1280-1430 meters. As the result, the depth trend analysis showed that if we considered the interface at shales overlies sand, both of shallow and deep sands have acoustic impedance of sands lower than shales represented as class 2 or class 3 according to Rutherford's AVO classification system. In AVO modeling, the two interested sand have intercept and gradient decreasing with angles and give negative reflection coefficient that corresponding with the previous analysis and the geology of the study area, However, the bed thicknesses in this study are mostly thinner than tuning thickness especially at deep depth.

ACKNOWLEDGMENT

I would like to express my gratitude to all those who gave me the possibility to complete this project. I would like to special thanks for Dr. Somchai Sriisaraporn from PTT Exploration & Production Public Co., Ltd. for giving me permission to commence this project in the first instance, to use departmental data and software. I have furthermore to thank my major advisor; Dr. Thanop Thitimakorn who spent his time gave knowledge and advices. He gave appreciate suggestion, checked and corrected the fault of this project. And my co-advisor, Ms. Orapan Limpornpipat from PTT Exploration & Production Public Co., Ltd. for all of comments and good suggestion. Also I would like to special thanks for all of teachers in department of geology, faculty of sciences, Chulalongkorn University for their instruction and knowledge throughout my four years in the university. Finally, my graduation would not be achieved without best wish from my parents who help me for everything and always gives me greatest love, willpower and financial support until this study completion. Also, thanks to my friends for their help and encouragement. Lastly, I offer my regards and blessings to all of those who supported me in any respect during the completion of the project.

CONTENTS

Introduction	
General statement	1
Problem define	7
Objections	7
Problem defined	7
Study area	8
Methodology	
Cross-plots	13
Fluids Replacement Modeling	17
Depth trend analysis	23
Synthetic AVO Gathers	26
Conclusion and Discussion	29
References	30

LIST OF TABLE

Table 1	The calculation of tuning thickness and limit of detectability of two sands formations	27
---------	--	----

LIST OF FIGURES

Figure1.1	The relationship of three key parameters rock properties, elastic moduli and acoustic properties.	2
Figure1.2.	Fluid effect on elastic properties and reflective coefficient respond to different fluids	3
Figure1.3.	Depth trend for sand and shale	4
Figure1.4.	Rutherford and William (1989) AVO classes for sand	6
Figure2.1	The study area is located in the western of S1 oilfield, Phitsanulok basin	8
Figure2.2	Cross-sections through the Phitsanulok Basin (Flint et al., 1988)	9
Figure2.3	Stratigraphy of the Phitsanulok Basin (Knox and Wakefield, 1983), in the red frame is highlight the formations that found in the study well.	10
Figure3.1	Cross-plotting of P-wave and S-wave velocities shows that a cluster of shale.	13
Figure3.2	Before and after generating new log in Chumsaengshales for top and base of wet sand, oil sand and gas sand, amplitude decrease with angle for the majority of the range	14
Figure3.3	Prediction Vs by set linear regression of Chumsaeng formation	15
Figure3.4	After editing log and predicting S-wave velocity (Vs)	15
Figure3.5	Cross-plotting Poisson's ratio with P-impedance	16
Figure3.6	Workflow of fluids replacement modeling	17
Figure 3.7	The lithology of two sands formations	18
Figure3.8	P-wave, density and AI against depth before replacing fluids	19
Figure3.9	P-wave, density and AI against depth were replaced by 100% of water.	20
Figure3.10	P-wave, density and AI against depth were replaced by 80% of gas	21

Figure3.11	P-wave, density and AI against depth were replaced by 80% of oil	22
Figure3.12	The factors controlled depth trend analysis	23
Figure3.13	The AI trends with different fluids; gas sands show the lowest AI Compareswith shales next below is oil and the water give nearest AI values with shales.	24
Figure3.14	The scatter of AI show good separation of sand and shale which sands have lower velocity than shales indicate AVO class 3	25
Figure3.15	The method of Synthetic AVO Gathers	26
Figure3.16	Left panel shows an extracted wavelet from full stack seismic. Right panel shows an amplitude spectrum in frequency domain.	26
Figure3.17	The shallow (A) and deep (B) sands formation of gas sands; oil sands and water sands represent the amplitude responses of top and bottom of sands.	28
Figure3.18	Measurement of amplitude with angle at shallow depth for top and base of wet sand, oil sand and gas sand, amplitude decrease with angle for the majority of the range	30
Figure3.19	Measurement of amplitude with angle at deep depth for top and base of wet sand, oil sand and gas sand, amplitude decrease with angle for the majority of the range	31

CHAPTER 1:INTRODUCTION

General statement

One of the primary goals is to define whether a water-saturated or a hydrocarbon-saturated causes the reflection of interest. It is necessary for the interpreter to understand the likely effects of lithology and fluid in order to identify the types of fluid fill from amplitude on seismic data. But before we can do so we need to have certain reasons for the correctness of amplitudes in the seismic data. Modeling the effect of fluids on the rock velocities and density is a basic method to ascertain the influence of pore fluids on seismic data. The technique of Rock physics and AVO are capable tools providing the link connecting seismic data, and to the presence of *insitu* hydrocarbon and to reservoir characteristics.

In this study, the interested amplitude anomalies will be studied by using well log data and analyze with the following techniques consists of Rock physics and AVO modeling. Rock physics technique will study about the relationship between the changing of physical properties of rock (lithology, rock frame, porosity, fluids and temperature), elastic properties (bulk and shear moduli) and acoustic properties (V_p , V_s , density). Workflow started with generating several cross-plots to observe the relation of the three key properties of rocks and to check quality of log data for editing; this process is the considerable parts to make the validity of amplitudes. While, fluid replacement modeling was created new log data of P-wave velocity, S-wave velocity and density after replacing with different fluids and calculating by Gassmann's equation (Gassmann, 2004). We interested in two sand formations at depth 868-878 m and 1280-1430 m. Using of Gassmann's equation it can be note that how the scatter of Acoustic Impedance (AI) values responses when changing fluids (Water, Gas and Oil). The output log data from replacement would be analyzed for AVO classification. And lastly, Synthetic AVO gathers were performed in order to model AVO responses in any particular geological environment at target depths by using Aki-Richard equations.

Theoretical background and Literature review

Rock physics is the study of the relationships between physical rockproperties, acoustic properties and seismic properties that depend largely on a combination of connectivity with elasticity and density of what is connected as shown in the figure1.1.

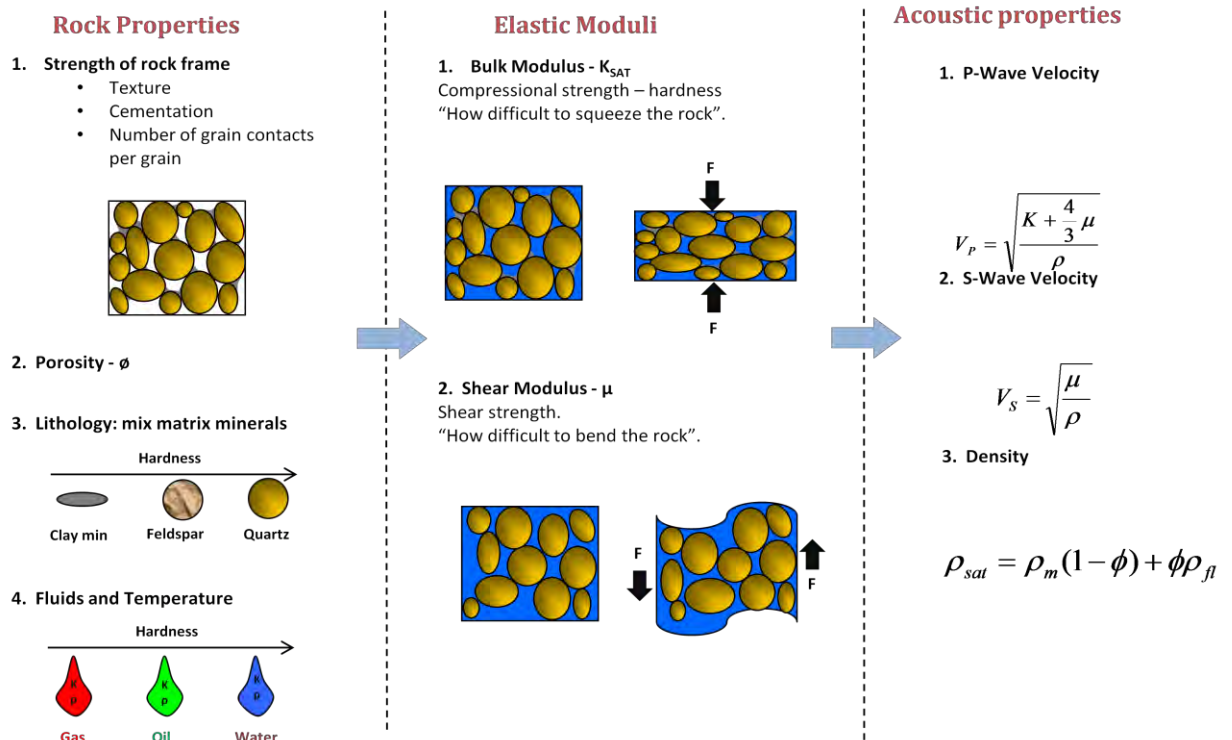


Figure 1.1 The relationship of three key parameters rock properties, elastic moduli and acoustic properties.

There are varieties of parameters that relate to the behavior of rocks in the term of stress. Two parameters that commonly refer to describe rock physics modeling are the bulk modulus and shear modulus. The bulk modulus controls the response of the rock to compressive stresses and indicates the extent of the rock that can be squashed. The shear modulus controls the response of a rock to shear translational stresses and indicates the rigidity of the rock. Bulk and shear moduli increase with compaction. A more easy way to understand the part of elastic moduli on the rock properties is to express them as parameters that are commonly measured like rock velocity and density. Furthermore, the three key parameters are required to understand AVO behavior including compression velocity, shear velocity and density. Compression velocities are related to particle displacement perpendicular to the direction of

wave motion. Rock bulk density is clearly the addition of the various density components (fluid and matrix).

Poisson's ratio is the ratio in of the proportional change in width to change in length for a uni-axial compression. It can be described as roles of the bulk and shear moduli and thus the P and S wave velocities. In AVO, Poisson's ratio is a significant parameter because the contrast of it across a boundary can have a large control on the rate of change of amplitude with offset. Some interpreters prefer to refer to the V_p/V_s ratio rather than Poisson's ratio. By the way, for most reasons it doesn't matter which parameter is used. To model seismic reflectivity, the acoustic impedance is mainly parameter which needs to refer. It is controlled by P-wave velocity and density (In practical term, describes when seismic wave are normal incident). The contrast of acoustic impedance across a boundary is an important affect on seismic reflectivity and expresses the reflection coefficient.

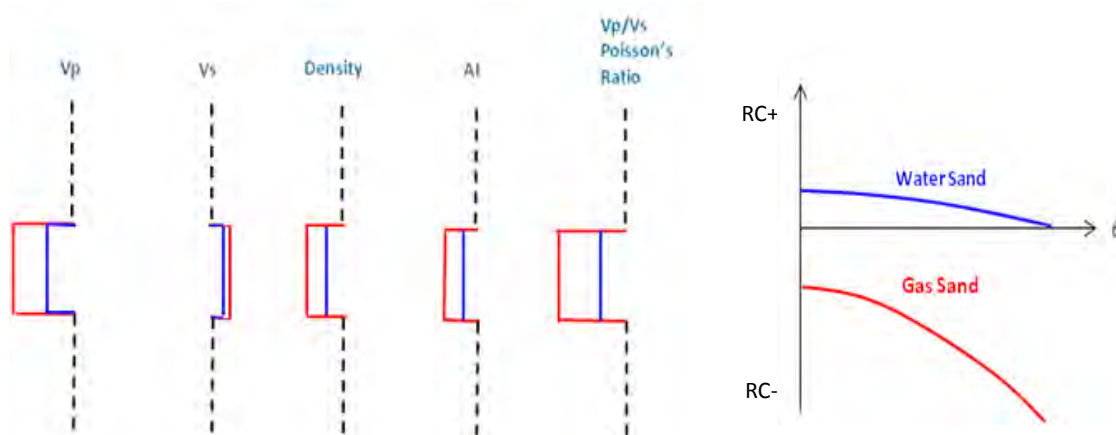


Figure 1.2. Fluid effect on elastic properties and reflective coefficient respond to different fluids

The contrast of elastic properties when different fluids in two interface layers shows that most of properties such V_p , density, and Poisson's ratio decrease with gas saturation. But, V_s is very insensitive to gas and provide little change in V_s . Poisson's ratio or V_p/V_s ratio are largely decreases with gas basically because the V_p change while the V_s does not. So, this is what the Reflection coefficient amplitude plot has shown (figure 1.3.). The intersection is defined by the contrast in acoustic impedance of two interface layer. Firstly, the water sand is defined by the difference in acoustic impedance which is positive so we get a small negative reflective coefficient. There is a small decrease in V_p/V_s , thus it provides a small AVO

gradient. For the gas sand it expresses a big negative contrast in acoustic impedance so, it gives a larger negative zero offset reflective coefficients and also a large negative change in V_p/V_s caused a large AVO gradient.

In case of fluid replacing model, Gassmann's Equation (Gassmann, 1951) has been used for calculating the effect of fluid substitution on seismic properties using the frame properties. It calculates the bulk modulus of a fluid saturated porous medium using the known bulk moduli of the solid matrix, the frame, and the pore fluid. For a rock, the solid matrix consists of rock-forming minerals, the frame refers to the skeleton rock sample, and the pore fluid can be gas, oil, water or a mixture of all three (Batzle and Wang, 2000). In oil and gas exploration, Gassmann's equations are used as seismic modeler. By the way, it is necessary to understand the limitation of Gassmann's equation for the accurate calculation. After modeling fluids, it is important to understand how the AVO respond related to elastic properties. A useful tool is the trend curve which illustrating the general relationship of the rock properties and lithology with depth.

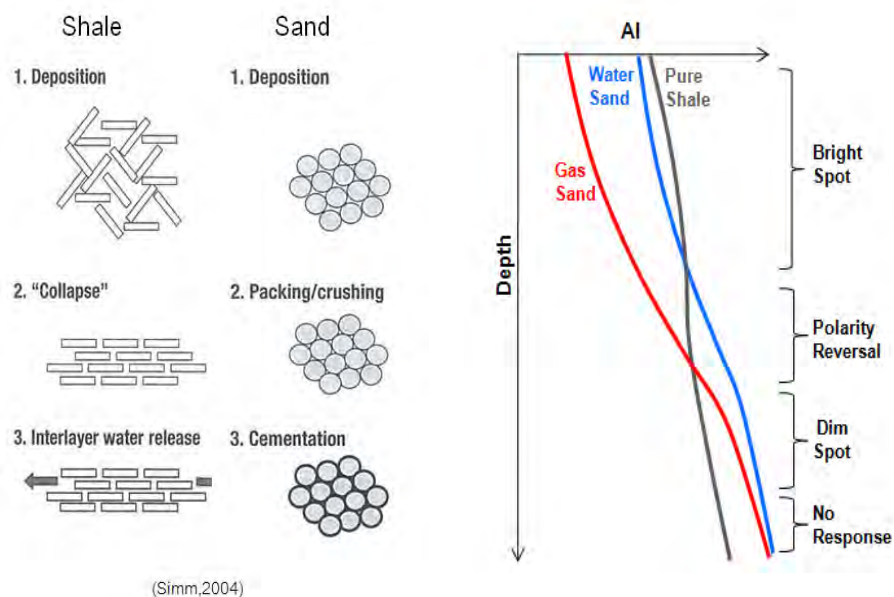


Figure 1.3. Depth trend for sand and shale

The depth trend analysis is to observe how the seismic signatures might change with depth. Owing to the acoustic properties change result from diagenesis that mainly because of compaction and cementation. A chart of porosity versus depth (Figure 1.3.) shows sand and

shale may be compacting at different rate. So, there are often several cross over in depth trend curves. This trend relates to the different mechanisms of porosity loss (as shown on the left of figure.1.3). The effect on acoustic properties increases with the porosity decreases and the rock become harden again giving cross over the trend of the AI curves. It is important to investigate if shale overlays sand, an interface is a positive or negative reflection coefficient because it may be changed depends on depth. The gas sand at the shallow depth has lower acoustic impedance than water sand but the gas effect reduces at deeper depth because of the rock hardens and porosity decreases. So we have to beware when the acoustic impedance of gas sand becomes higher at the depth that gas sand relative to water sand and shale. Since the amplitude signature of gas sand will vary with depth, it is very important for the amplitude interpretation. Such gas sand in the shallow may seem to giving a bright spot on seismic. However, it shows a polarity reversal and a dim spot if the sand is harder than the shale.

Seismic reflections from gas sands exhibit a wide range of amplitude-versus-offset (AVO) characteristics. The two factors that mostly strongly determine the AVO behavior of a gas sand reflection are the normal incident reflection coefficient R_0 and the contrast in Poisson's ratio at the reflector. Using of the AVO plots in interpretation is the feature of different types of response, depending on lithology and fluid type. Rutherford and Williams (1989) classified shale/brine sand AVA (Amplitude versus angle) responses into three types (I, II & III) depending to the impedance contrast between the shale and the sand. Type I responses are characterized by a positive contrast in impedance, together with a decreasing amplitude with angle. Class II responses have small normal incident amplitudes (positive or negative), but the AVO effect leads to high negative amplitudes at far offset.

Ross and Kinman (1995) have suggested that the small positive class II responses should be termed Class IIp, owing to the phase reversal that is inherent in these responses. Class III responses have large negative impedance contrasts and the negative gradient leads to increasing amplitude with angle (see figure 1.4).

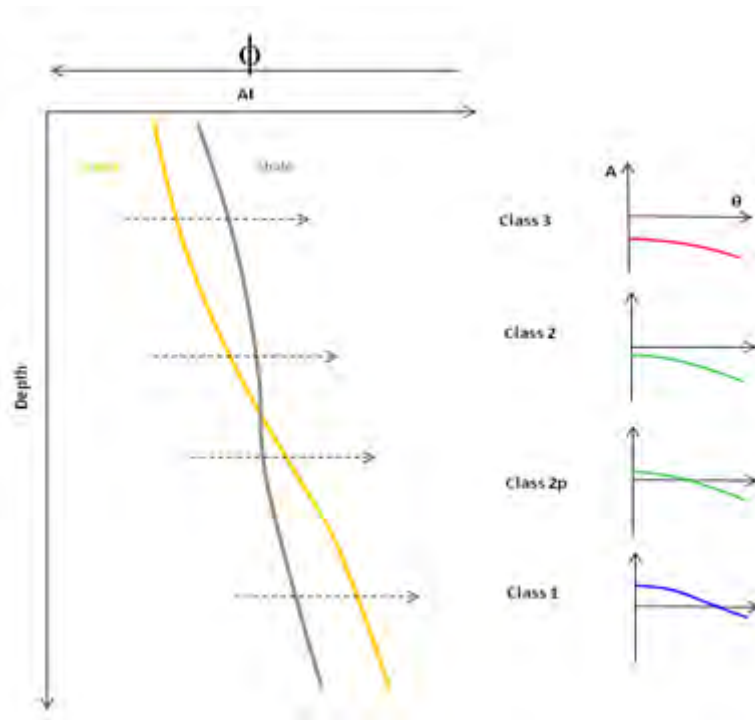


Figure 1.4. Rutherford and William (1989) AVO classes for sand

Synthetic seismogram gathers were generated to observe the theoretical AVO responses for gas, oil and water sands at different thicknesses. Angles were calculated for different offsets by ray-tracing and then Aki-Richard's equation used to calculate reflection coefficients.

A more readily understandable approximation was derived by Aki and Richard (1980) and this is shown in Equation 1. The approximation comprises 3 terms, with the 'A' term being the zero angle reflection coefficient related to the contrast of acoustic impedance. The non-zero offset component of the reflectivity is given by 'B' and 'C' terms.

$$R(\theta) = A + B \sin^2(\theta) + C \sin^2(\theta) \tan^2(\theta) \quad (1)$$

While;

$$A = \frac{1}{2} \left(\frac{\Delta V_p}{V_p} + \frac{\Delta \rho}{\rho} \right) \quad \text{Zero angle of Impedance } R_0 = \frac{V_{p2} \rho_2 - V_{p1} \rho_1}{V_{p2} \rho_2 + V_{p1} \rho_1}$$

$$B = \frac{\Delta V_p}{2V_p} - 4 \left(\frac{V_s}{V_p} \right)^2 \left(\frac{\Delta V_s}{V_s} \right) - 2 \left(\frac{V_s}{V_p} \right)^2 \frac{\Delta \rho}{\rho}$$

$$C = \frac{1}{2} \frac{\Delta V_p}{V_p}$$

Non-zero components

Problem Defined

Seismic amplitude anomalies are useful hydrocarbon indicators for the interpreters however they may be caused by many reasons.

Hypothesis

The amplitude anomalies caused by gas sand and have AVO class 3.

Scope of work

The data used this study are consist of well log data from Sirikit field, Pitsanulok Basin and analyzed by using Hampson-Russell software in order to generate cross-plotting, fluid replacement model and synthetic seismogram gather. Depth trend analysis are performed by Microsoft excel.

CHAPTER 2: STUDY AREA

The Phitsanulok Basin is the largest oilfield onshore Thailand, holding close to one third of oil reserves in the country. The Phitsanulok Basin is one of a series of Cenozoic Tertiary rift-related basins. Approximately the area lines 400 kilometers north of Bangkok. The study area located onshore in Nong Plueng area, western Sirikit Oilfield, Kamphaengphet province.



Figure 2.1 the study area is located in the western of S1 oilfield, Phitsanulok basin

The study area stratigraphic units are contains fluvial sandstones of the Middle-Upper Miocene Pradu Tao and Yom Formations (Chuenbunchom et al., 2003)that overlies lacustrine shales of the Chum Saeng Formation.

The Pradu Tao Formation is ~300 m thick and shale divides it into two units termed UPTO and LPTO. Similarly, the Yom Formation is ~250 m thick and a 5-30 m-thick shale divides it into two units named UYOM and LYOM. The typical thickness of stacked, fluvial channel sandstone bodies in the Lower Pradu Tao. In the Upper Pradu Tao the bodies are less well connected and are 5-10 m thick. Sandstone bodies in the Lower Yom are typically 2-5 m thick and isolated.

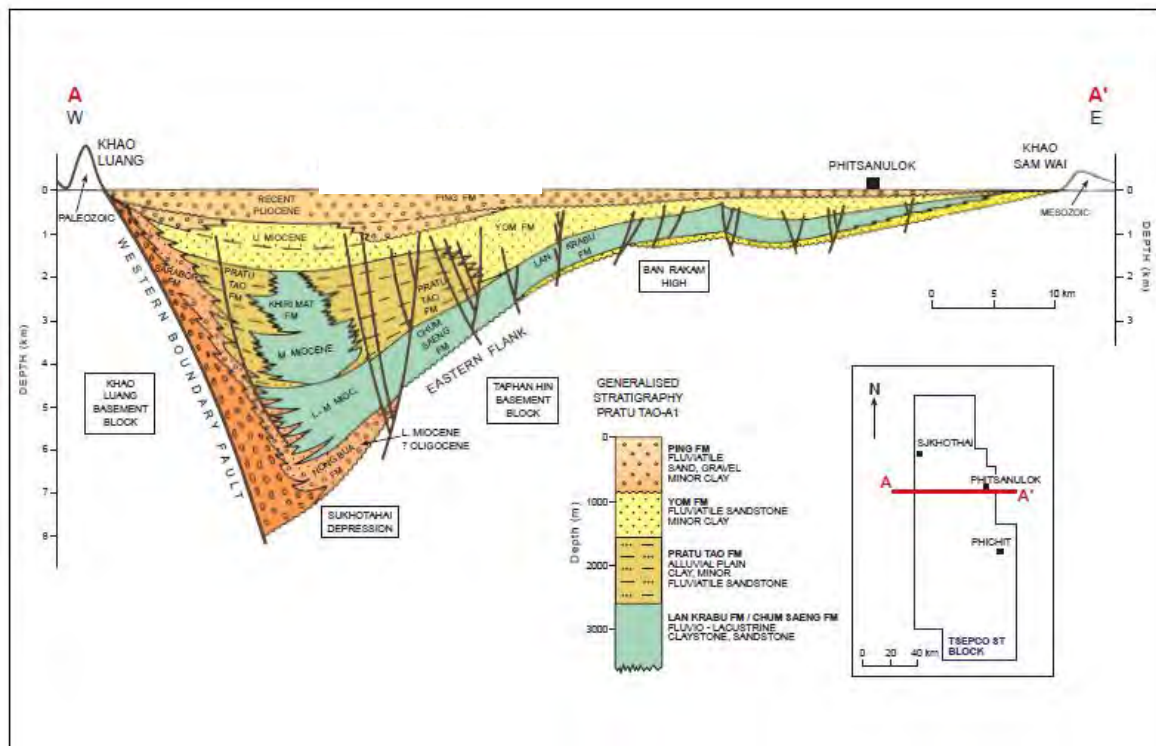
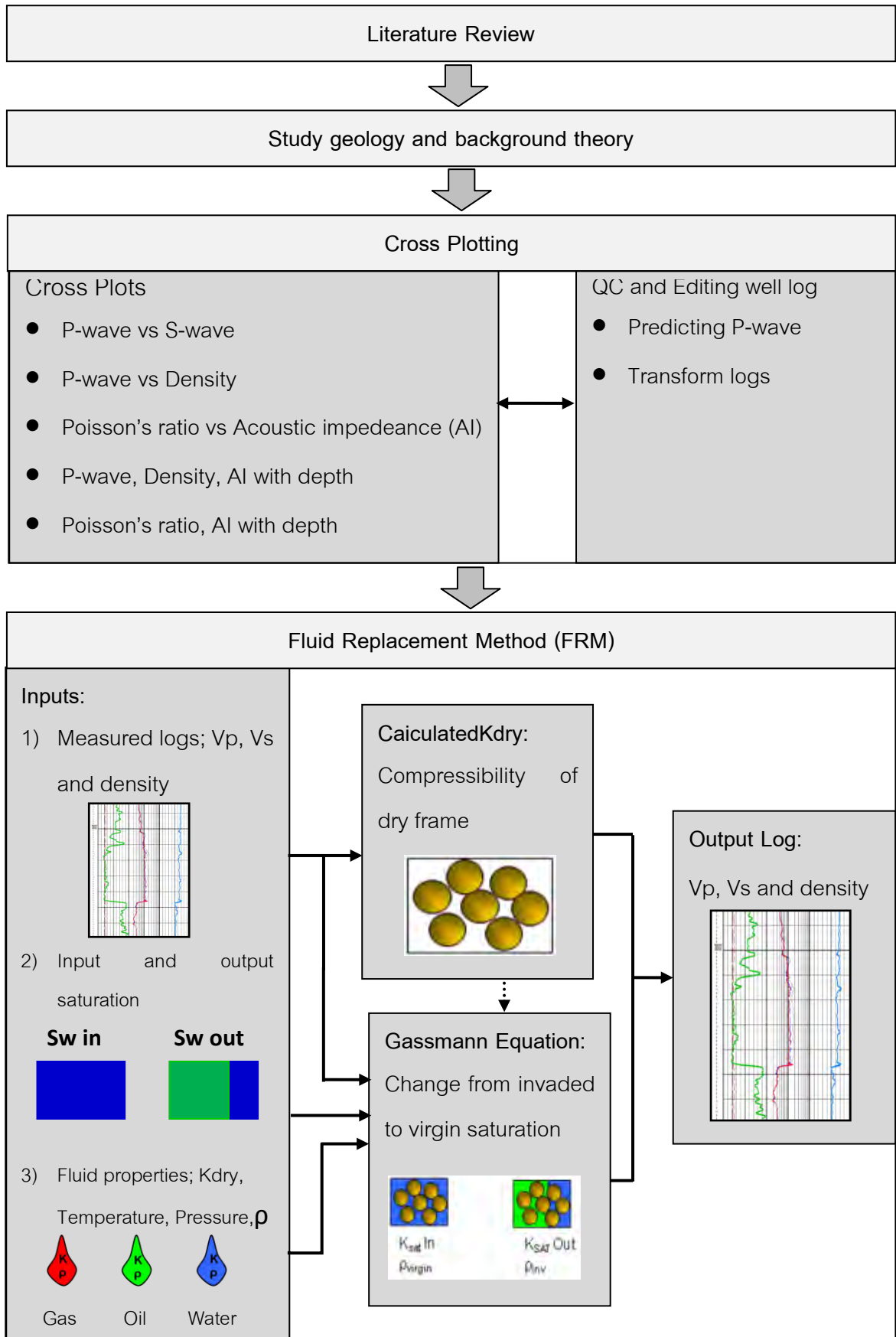


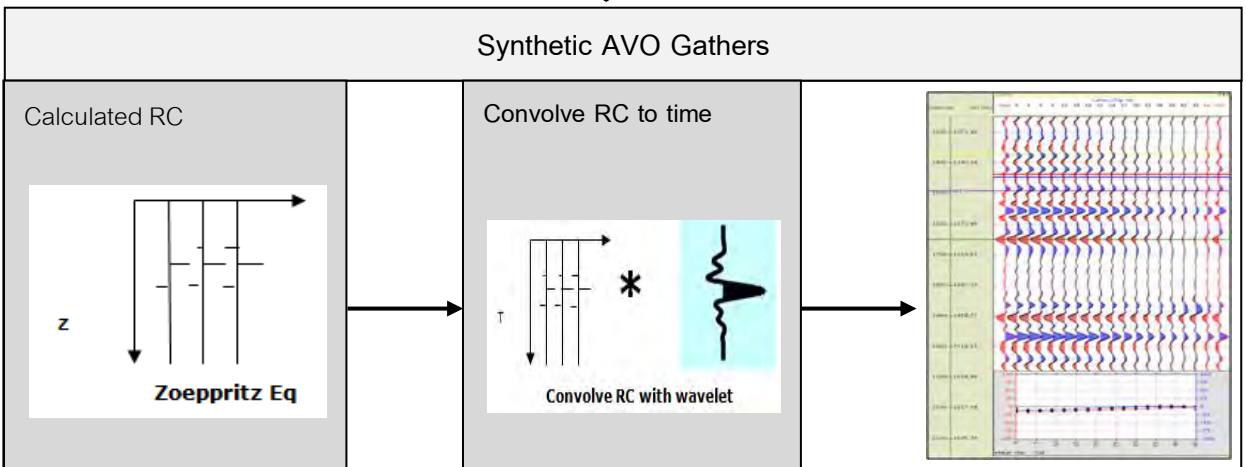
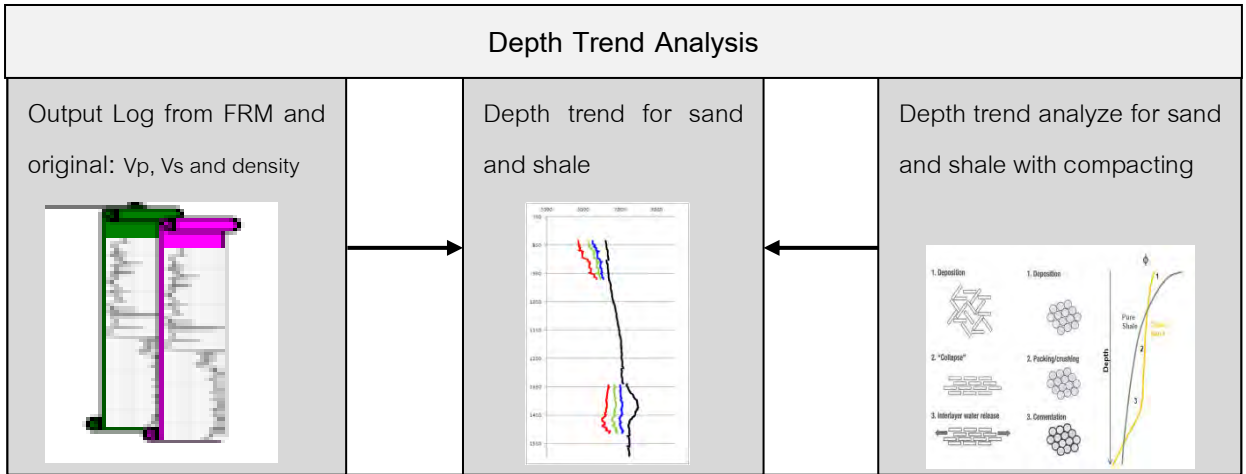
Figure 2.2 Cross-sections through the Phitsanulok Basin (Flint et al., 1988)

AGE	FORMATION	THICKNESS (UP TO)	LITHOLOGY	DESCRIPTION	ENVIRONMENT
LATE MIOCENE - RECENT	PING	1,300 m		SANDS/GRAVELS WITH ASSOCIATED CLAYS Sands, clear, white, coarse grained, occasionally gravel. Gravels, variegated, lithic Clays, varicoloured, sandy, silty	Alluvial Fan & Alluvial Plain
MIDDLE MIOCENE - LATE MIOCENE	YOM	1,600 m		SANDS/CLAYS Sands, clear, white, coarse grained, occasionally gravel. Clays, varicoloured, sandy, silty	Fluvial
	PRATU TAO	2,200 m		SAND (STONES)/CLAY (STONES) Sand (stones), clear, white, fine-coarse grained Clay (stones), redbrown, varicoloured, sandy, silty	Ephemeral Lacustrine & Fluvial
EARLY MIOCENE - MIDDLE MIOCENE	LANKRABU - CHUM SAENG	2,200 m		CLAYSTONES AND SILTSTONES/SANDSTONES Claystones and siltstones, grey, silty, occasionally gastropod-bearing and carbonaceous Sandstones, clear, white, grey, fine-medium grained, thinly bedded	Lacustrine & Fluvialacustrine
OLIGOCENE - EARLY MIOCENE	SARABOP - NONG BUA	1,200 m		CLAYSTONES Claystones, redbrown, occasionally grey to varicoloured, with minor coarse-fine lithic sandstones	Fluvial & Ephemeral Lacustrine
PRE-TERTIARY BASEMENT				MESOZOIC - PALEOZOIC CLASTIC, CARBONATE, VOLCANICLASTIC IGNEOUS, AND METAMORPHIC ROCKS	

Figure 2.3 Stratigraphy of the Phitsanulok Basin (Knox and Wakefield, 1983), in the red frame is highlight the formations that found in the study well.

CHAPTER 3: METHODOLOGY





I. Cross-plots

The initial rock physics analysis on log data is to compare cross-plots of the key parameters. The cross-plot of V_p and V_s represents lithology of gas sand, water sand, oil sand and shale. V_p is around 850 – 2100 m/s and V_s are approximately 1900-4100 m/s. Obviously, gas sand separate from shale trend and water sand as water sand are have slightly lower V_p than shale. Moreover, there were some points that dispersed from the main trend. This group of points was shown in log data as spikes or peaks in both V_p and V_s . These spikes or peaks have to be edited out from log data since because it may cause the ambiguity when calculated Gassman's equation and generated AVO modeling. Furthermore, there are a cluster of shale in the red circle that has very low V_p (Figure 3.1).

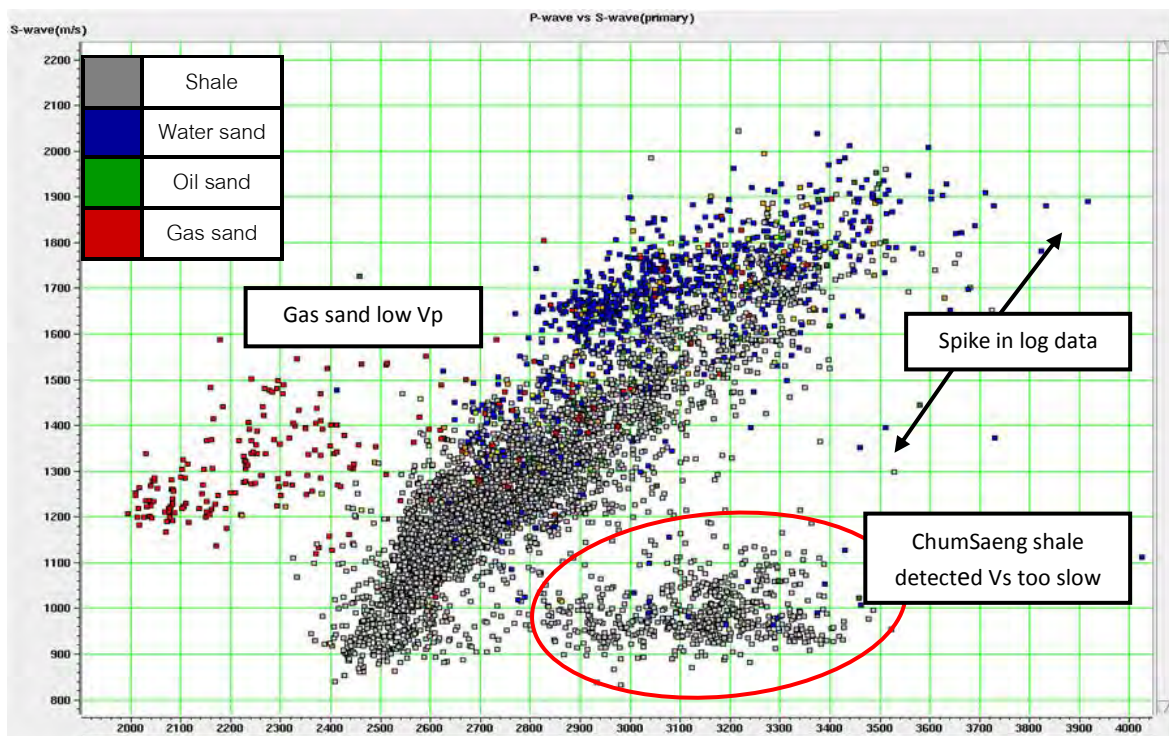


Figure3.1 Cross-plotting of P-wave and S-wave velocities shows that a cluster of shale in red circle has S-wave velocity very low(V_s) compare to P-wave velocity (V_p)

Normally, V_s should be approximately half of V_p at the shallow depth and a bit lower with increasing depth (Castagna, 1982) but from cross-plots V_p of these shale range from 2900 to 3400 m/s while V_s is only around 900-1100 m/s. This caused the ratio of V_p to V_s (V_p/V_s). This effect may arise from an error during borehole measurement because this

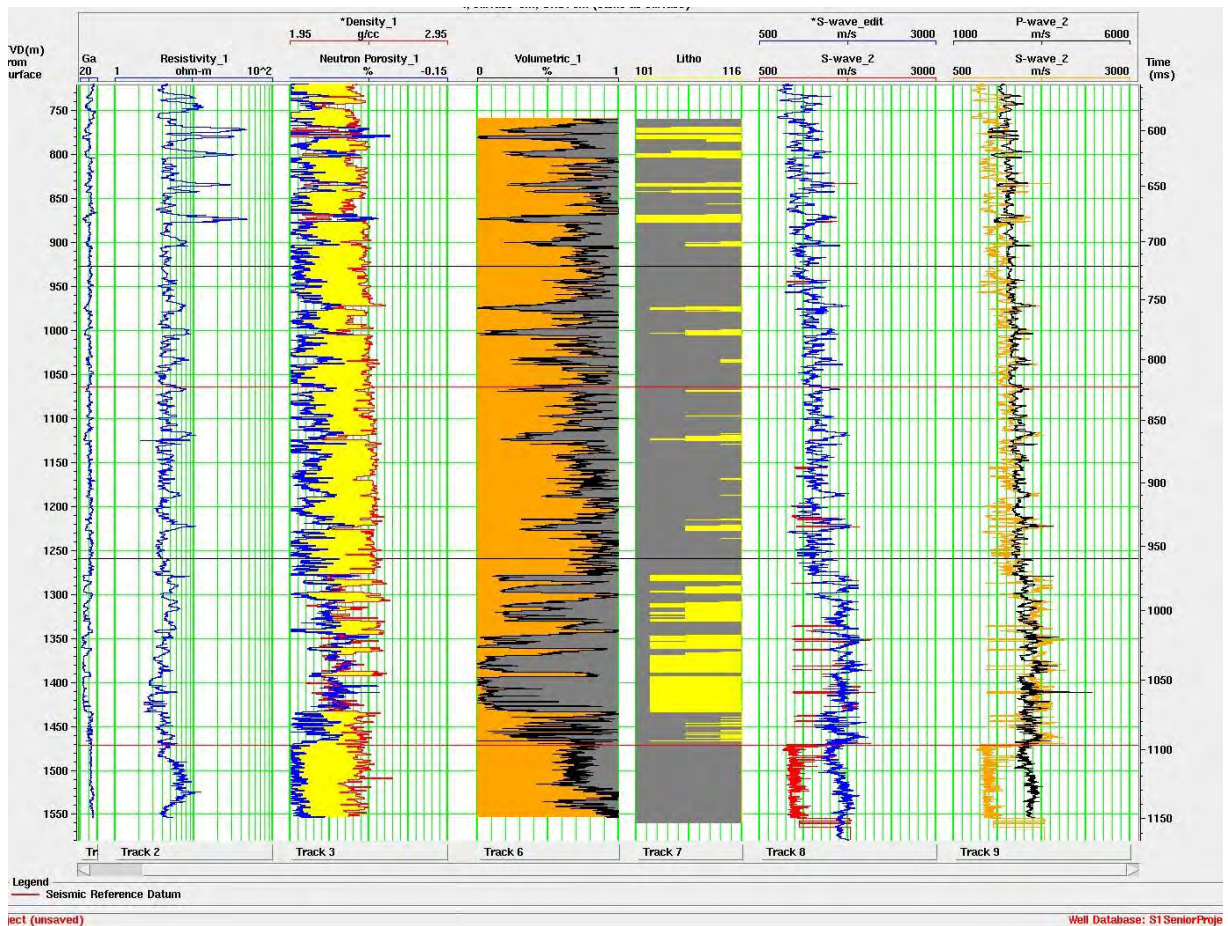


Figure 3.2 Before and after generating new log in Chumsaeng shale and comparing both of V_p and V_s with other logs.

shale were represented as Chumsaeng formation which deposited in Lacustrine environment make them had very slow velocity due to higher content of organic matter. V_s prediction was the necessary thing to do because we have to use it in order to calculate as Poisson's ratio or V_p/V_s ratio for observe the change of elastic properties due to fluids and lithology. To predict V_s we first have to cross plot V_p versus V_s of Chumsaeng formation from nearly well in order to set linear equation (Greenburg and Castagna, 1992) then transform V_p into V_s by using the coefficient according to linear equation (Figure 3.3).

Finally, when plotting P-wave and S-wave velocities after predicted V_s and edited log data it had shown that the cluster of shale and spike log data was disappear (Figure 3.4).

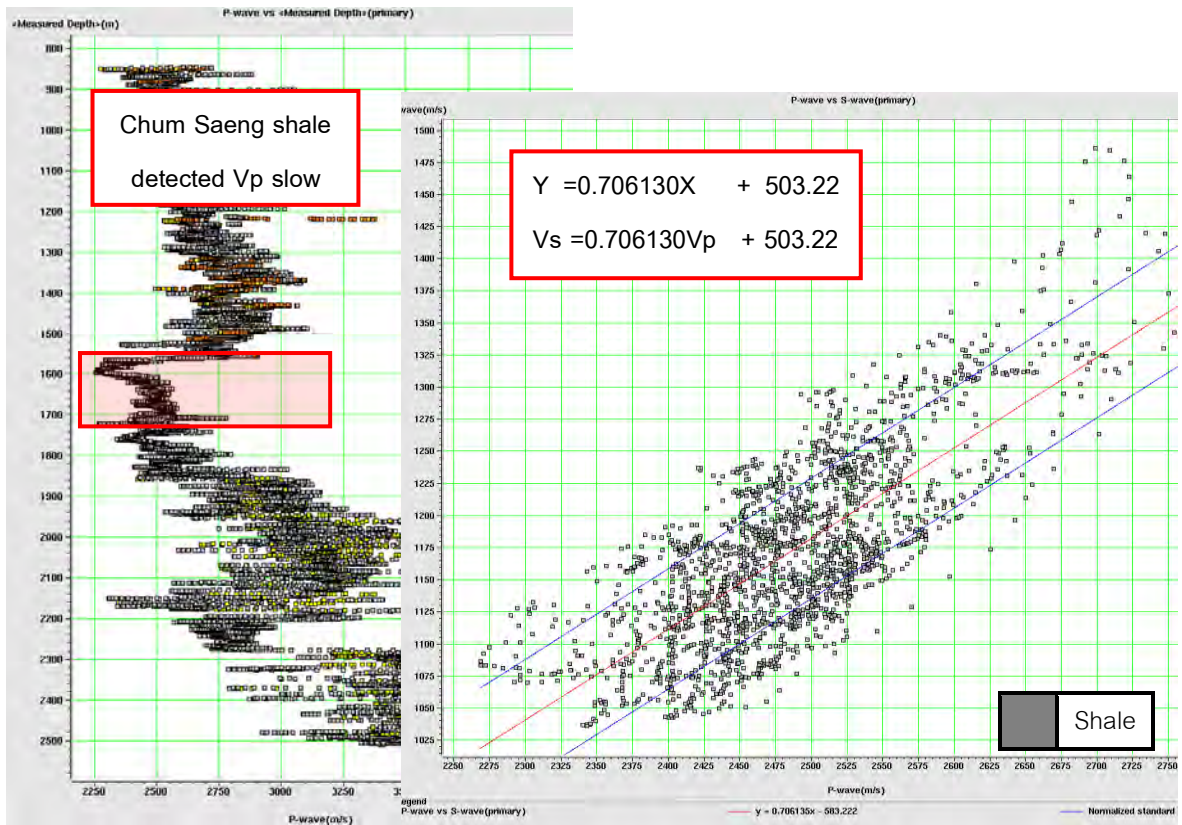


Figure3.3 Prediction of Vs by linear regression of Chumsaeng formation from another well.

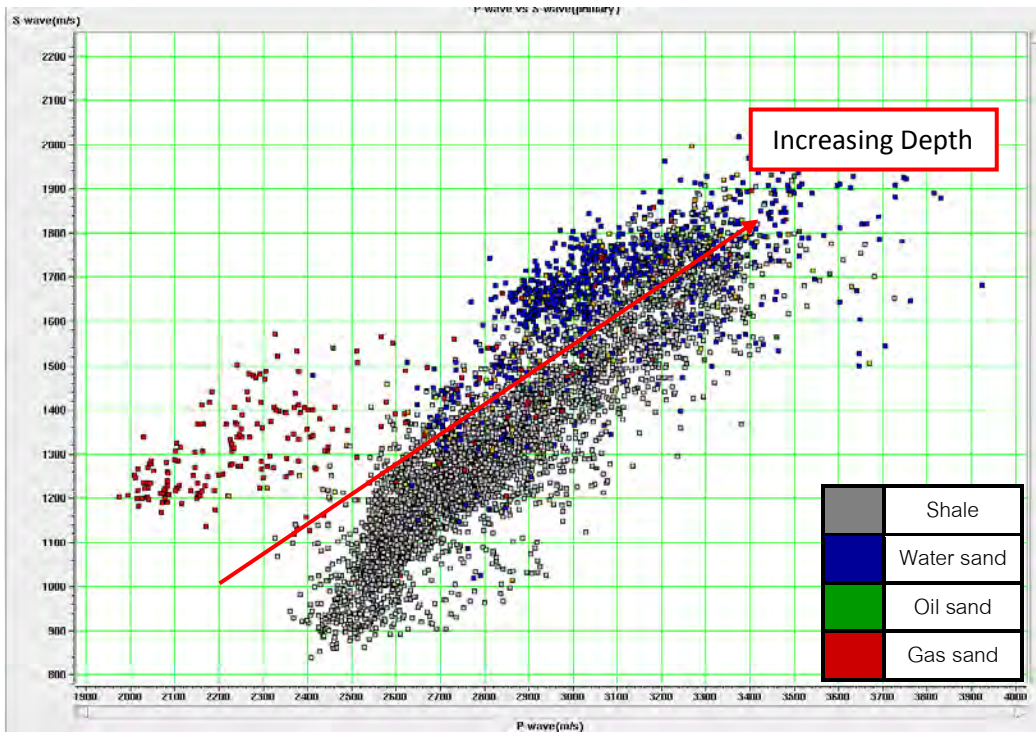


Figure3.4 After editing log and predicting S-wave velocity (Vs)

With several cross-plots, gas sand has lower P-wave velocity than water sand, oil sand and shale while gas sand, water sand, oil sand and shale have density increasing respectively. As, there were a small number of oil sand so they might hard to notice. Acoustic impedance of gas sand will be lower than water sand and oil sand as well(Figure 3.5). Gas sand has very low acoustic impedance and give high contrast with water sand, oil sand and shale, but their Poisson's ratio still has some overlap with water sand.

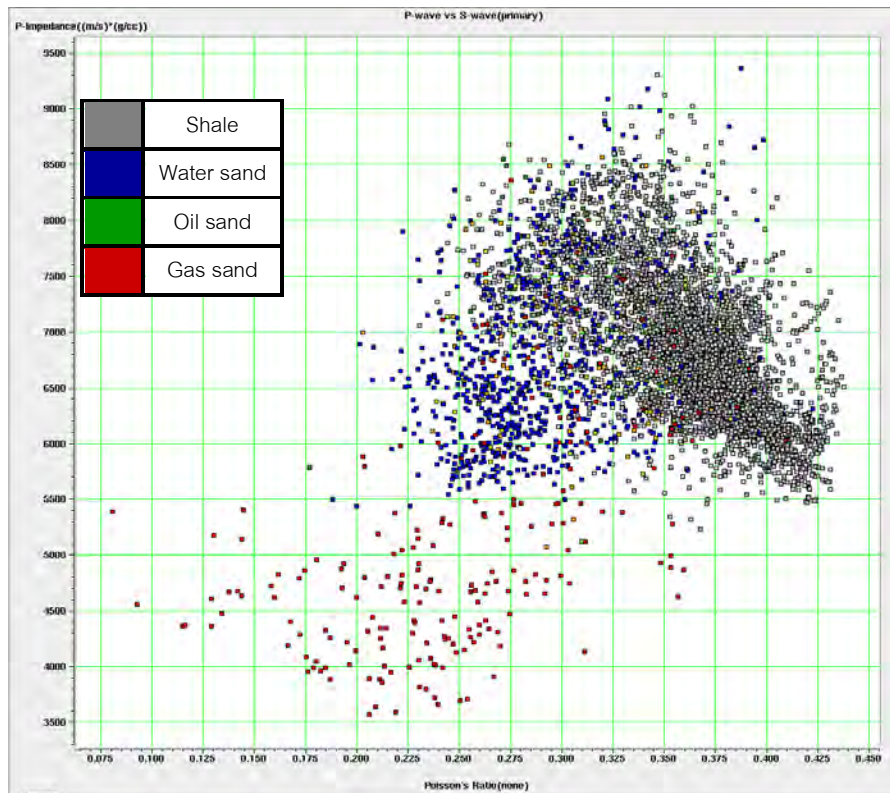


Figure 3.5 Cross-plotting Poisson's ratio with P-impedance

At shallow depth gas sand has very low acoustic impedance and high contrast with shale. While acoustic impedance at the deeper depth has very low contrast of water sand and shale. An important observation is that there is a general trend of increasing acoustic impedance with depth. This is the normal compaction trend related to the decreasing porosity with increased depth. Moreover, with the low distinct of acoustic impedance demonstrates that only acoustic impedance cannot define lithology. However, Poisson's ratio or V_p/V_s still shows good contrast of water sand and shale still is the best parameter for separating lithology at all depths (Figure 3.5).

II. Fluids Replacement Modeling

In this case, fluid replacement model (FRM) was generated in order to observe the change of acoustic properties due to fluids substitution. The first inputs data are the edited Vp, Vs and density logs. Secondly, measured water saturation and outputs saturation were input with three conditions; 100% of water, 80% of gas and 80% of oil. The last inputs are the data of temperature, pressure, fluids density to calculate fluid properties correspond with reality. After that, software would be calculated K_{dry} then the Gassmann's equation would be change invaded into virgin zone to model the new out fluids. Finally, we got the new logs with three kinds of fluids (Figure 3.6).

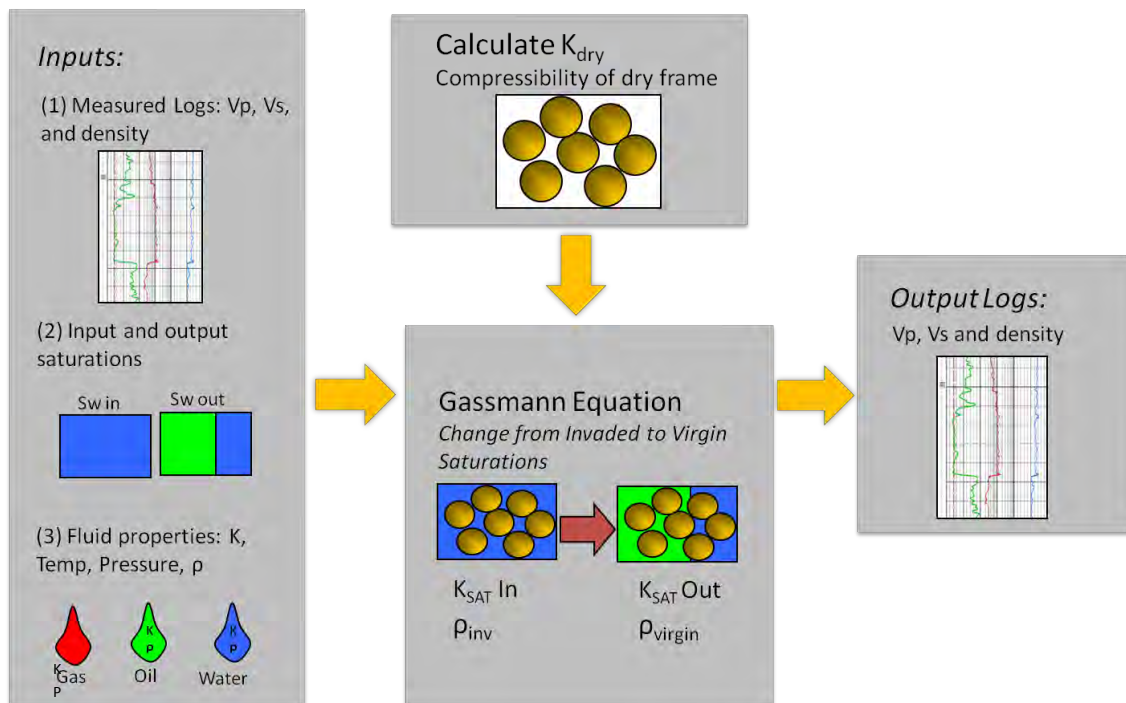


Figure 3.6 Workflow of fluids replacement modeling

In this study, we were interested in two sand formations that providing enough sand data to calculate where at the depths 868-878 m. and 1280-1430 m. The interested formations were replaced by three different cases of fluids. At the shallow depth, the input logs are contain amount of gas sands so the fluids replacement started by substituted these gas with water 100% then 80% of oil respectively. While water sands at the deep depth are replaced with gas 80% and oil 80%. As a result, with water 100% both of two sand formations

have the highest Vp, density, AI and Poisson's ratio compare to oil 80% and gas 80%. Accordingly, the model of gas and oil shows P-wave, density, AI and Poisson's ratio are more decreasing respectively. Moreover, the deep formation with 80% of gas is obvious that P-wave, density, AI and Poisson's ratio are all decreasing and clearly separate from shale trends. Especially, Poisson's ratio displays good contrast of sand and shale in both hydrocarbon cases (Figure 3.9, Figure 3.10 and Figure 3.11).

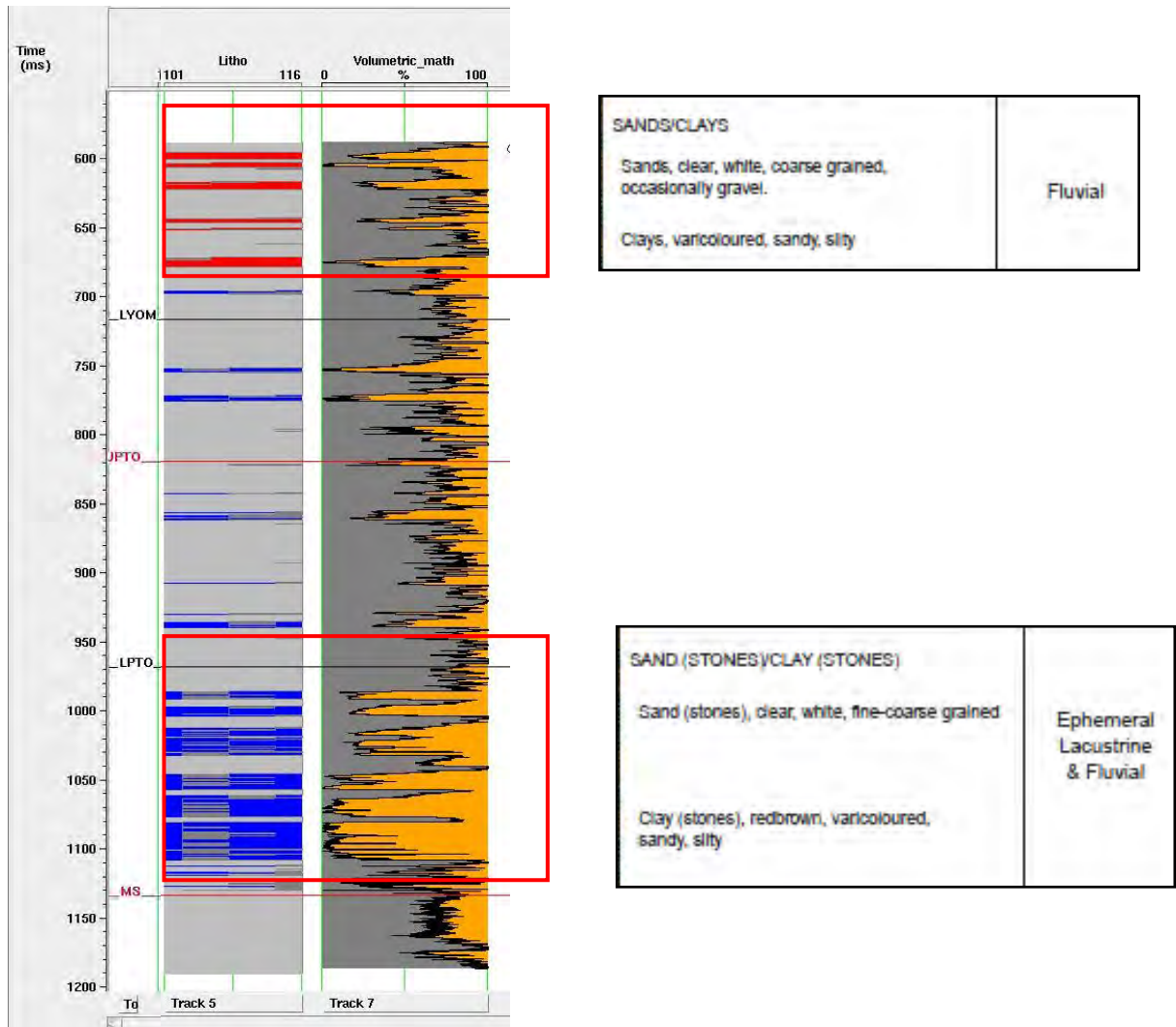


Figure 3.7 The lithology of two sands formations

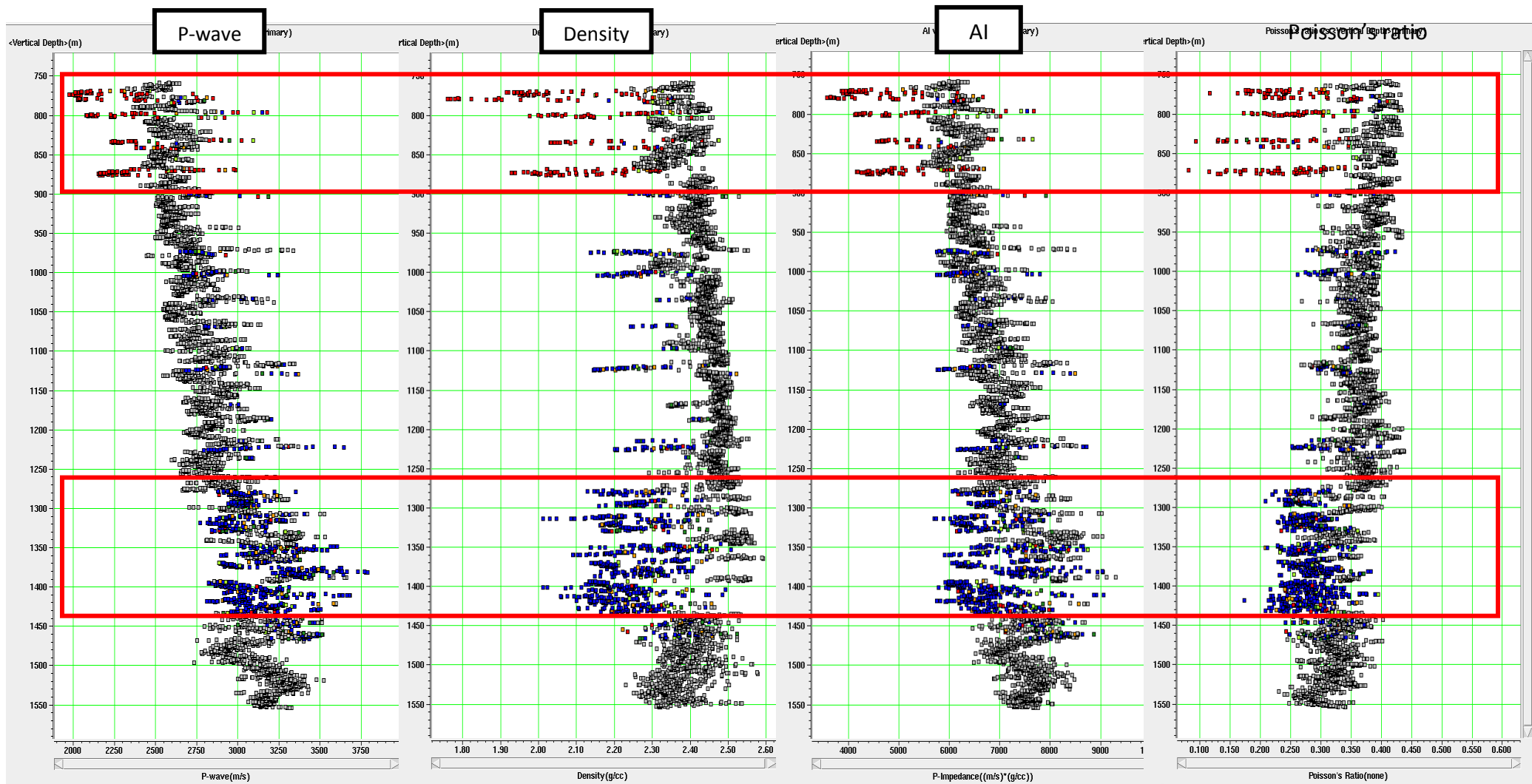


Figure 3.8 P-wave, density and AI against depth before replaced fluids.

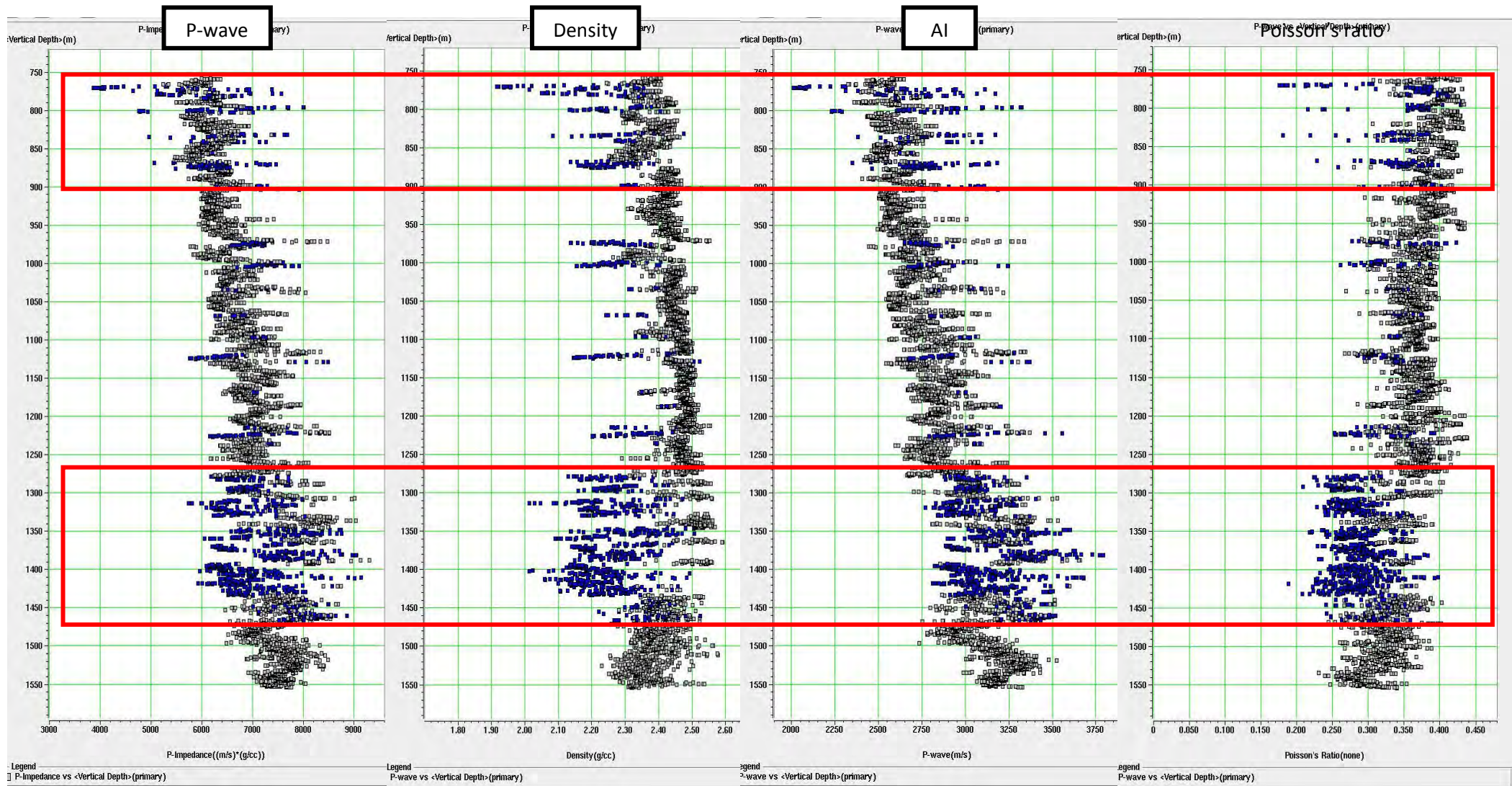


Figure3.9 P-wave, density and AI against depth were replaced by 100% of water.

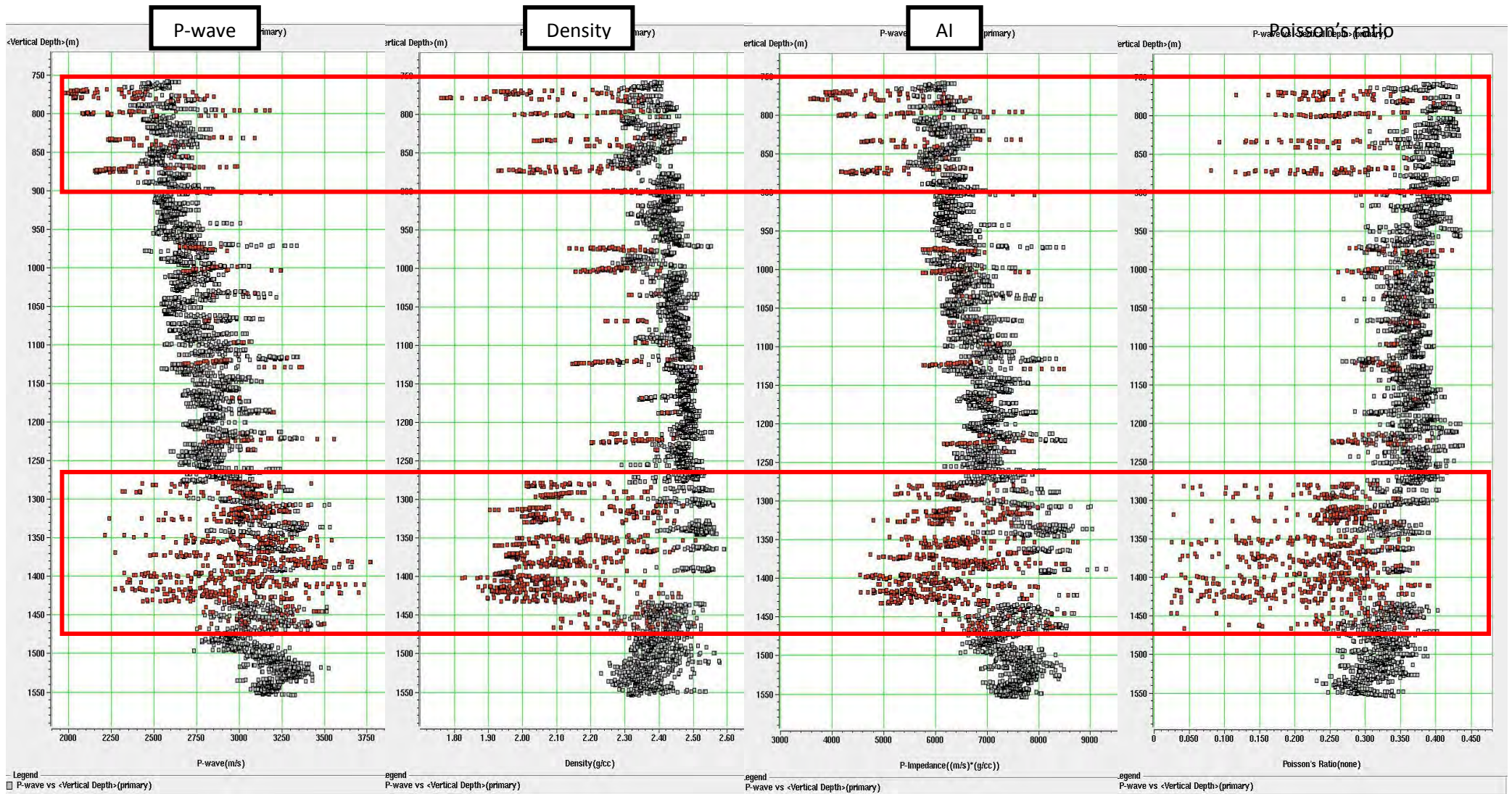


Figure3.10 P-wave, density and AI against depth was replaced by 80% of gas

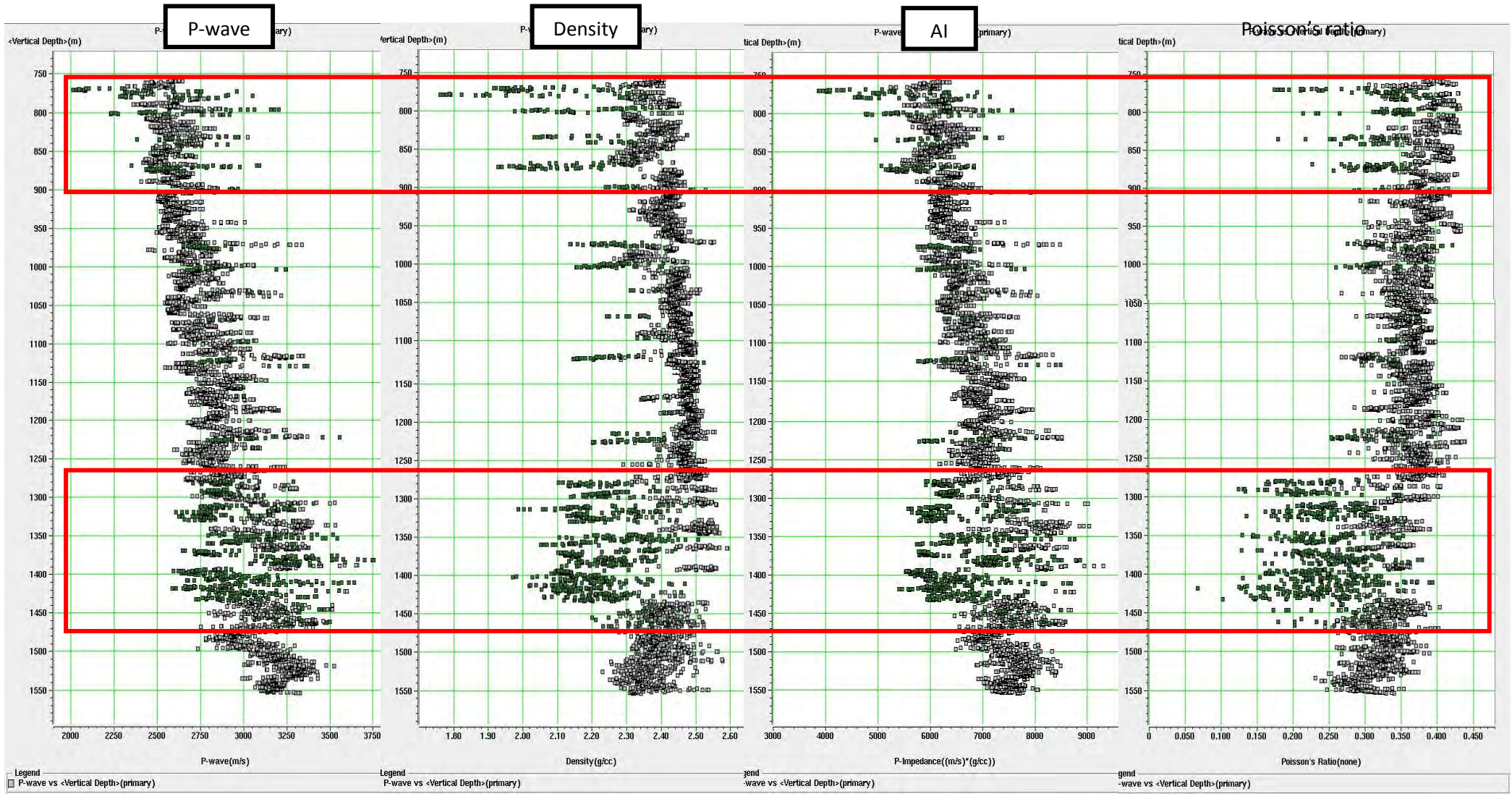


Figure 3.11 P-wave, density and AI against depth were replaced by 80% of oil.

III. Depth Trend Analysis

The depth trends analysis is performed to see how the seismic signatures might change with depth by observing the acoustic impedance values. The reason is that the change of acoustic impedance is mainly due to compaction and cementation. From a plot of porosity versus depth (Figure 3.12) it's shown that sands and shales are compacted at different rates, they are often show crossovers in the trend curves which relate to the different mechanisms of porosity loss (as shown on the left of figure 3.12). When the porosity decreases and the rock hardens, acoustic properties (AI) will increase and there may be crossovers. So it is important to investigate whether the interface of shale over sand is a positive or negative reflection coefficient in which they may change with depth. Importantly, if the gas sand is also represented, AI trends of gas sands are lower than water sand however the gas effect reduces with depth as the rock hardens and porosity decrease. At the position of AI water and gas relative to shale and the amplitude signature of gas sand will vary with depth. This depth dependency is very important for our amplitude interpretation, at the shallow depth; the gas is likely to show a bright spot on seismic data. However, we can see a polarity reversal and a dim spot if the sand is harder than the shale. Of course if the fluid effect is small there will be no fluid response on amplitude.

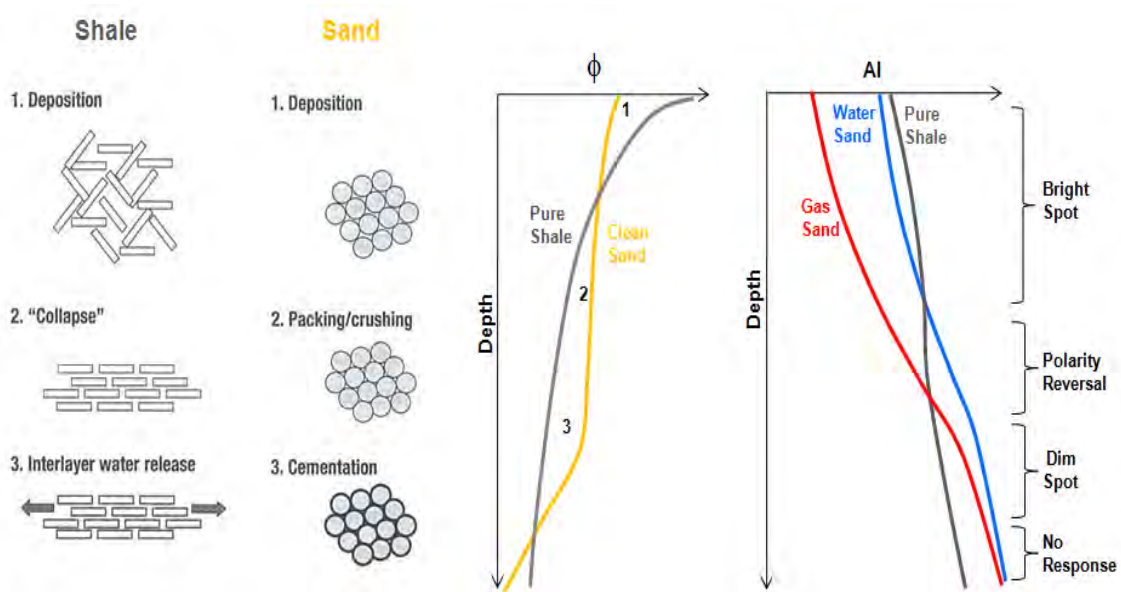
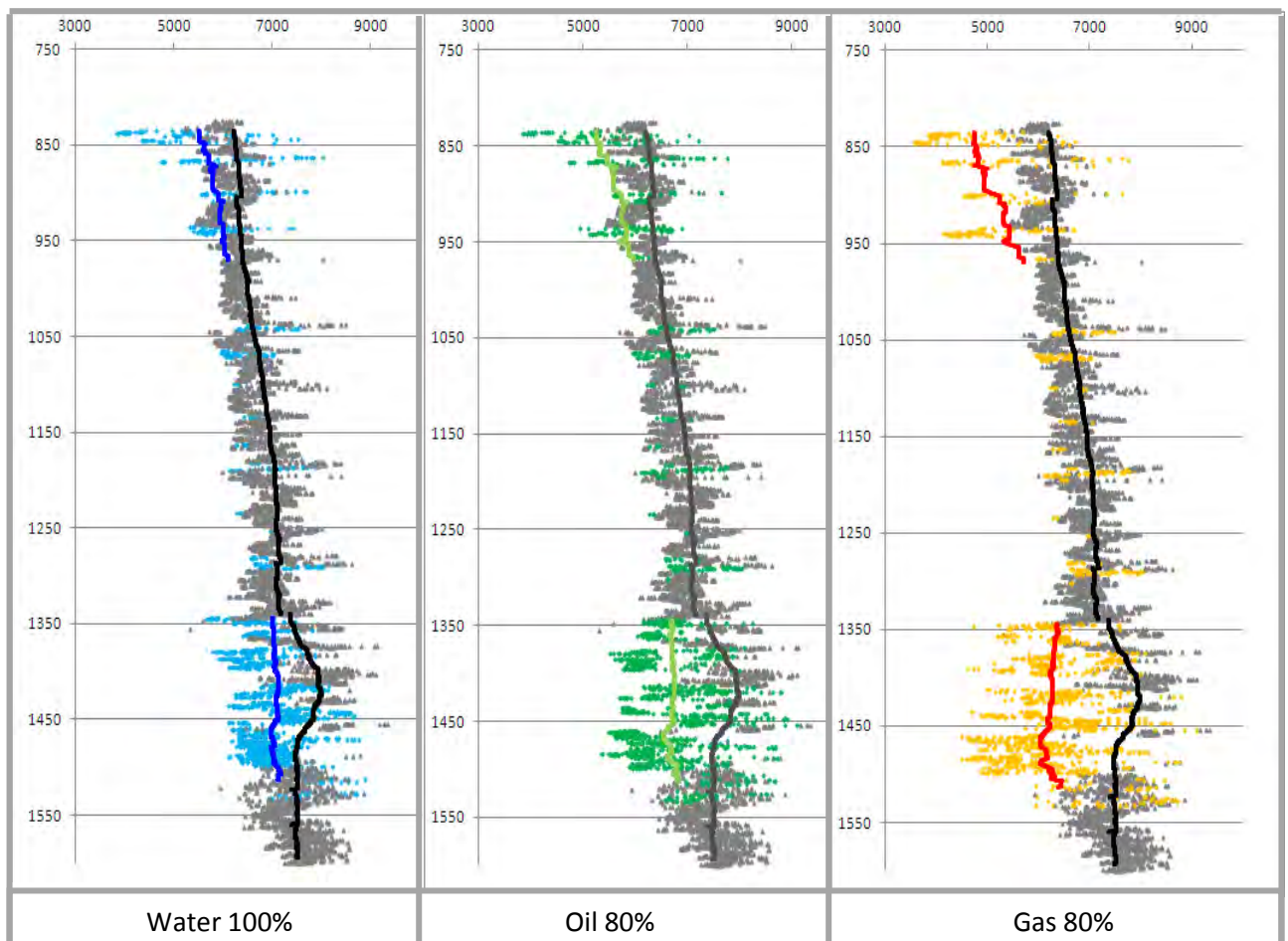
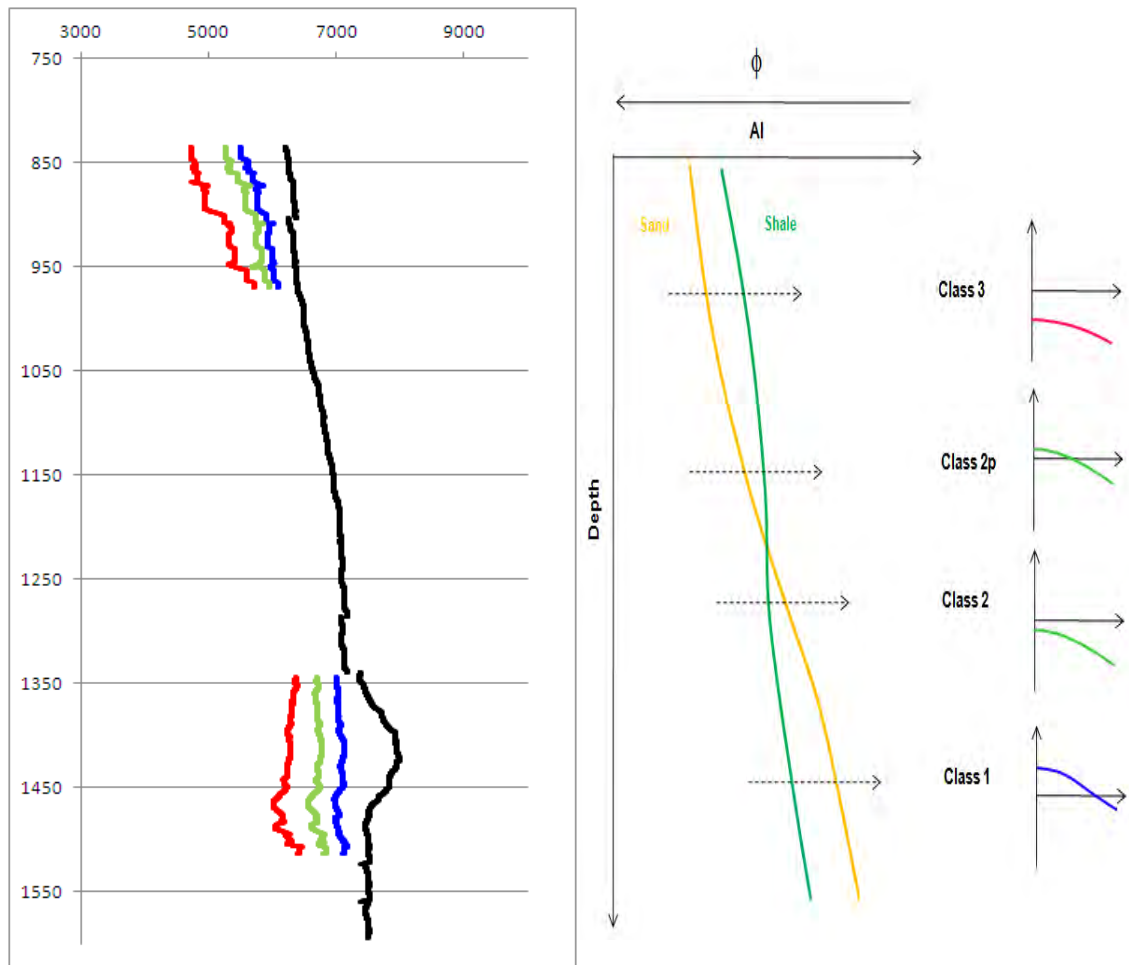


Figure 3.12 The factors controlled depth trend analysis

Owing to the fluids replacement models, the output data of P-wave velocities and density of sands with gas 80%, oil 80% and water 100% were calculated as the Acoustic impedance. The spread of AI values was analyzed to see if AI change was mainly because of lithology variation, fluids type or other reservoir properties. AI variation explains the significance of amplitude variation observed on the near offset stack. To classify AVO classification is to compare AI trends of gas sand; oil sand and water sand with the AI trends of shale which the results are all shown as class 2 or class 3. The class 3 of AVO indicates that sand and shale have low compaction in this study while sand has high porosity cause AI of sand lower than shale. While, the class 2 of AVO indicates that sand and shale have a little higher compact than class 3. So, the AVO class 2 and 3 are hardly to identify.



The figure 3.13 The AI trends with different fluids; gas sands show the lowest AI compares with shales next below is oil and the water give nearest AI values with shales.



The figure 3.14 The scatter of ϕ show good separation of sand and shale which sands have lower velocity than shales indicate AVO class 3 (Rutherford and William, 1989)

IV. Synthetic AVO Gathers

Synthetic AVO Gathers are calculated by using Aki-Richard equation to calculate RC for seismic traces at different angles and convert to time then convolve with our wavelet.

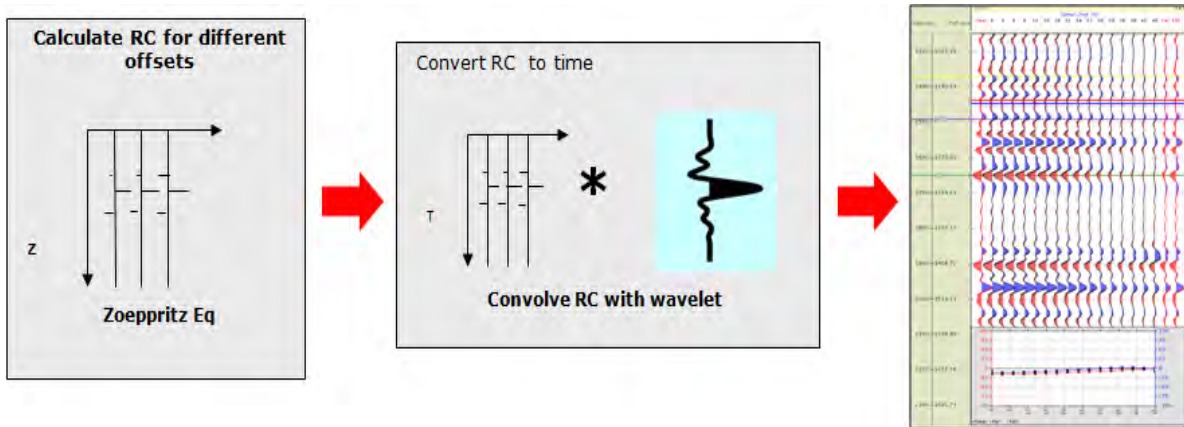


Figure 3.15 The method of Synthetic AVO Gathers

But before performing synthetic AVO gathers, it's important to find tuning thicknesses and limit of detectability. Tuning thickness and limit of detectability can then be calculated and compared with the observed reservoir thicknesses at different depths using frequency information extracted from the full stack seismic and dominant frequency measured from the amplitude spectrum and the velocities of sands were obtained from well log information so the wavelength could be calculated. In this study, we assumed that the acoustic impedance of reservoir and seal were conducive to yielding an AVO response, AVO as only expected to work more reliably for reservoirs greater than and equal to tuning thickness.

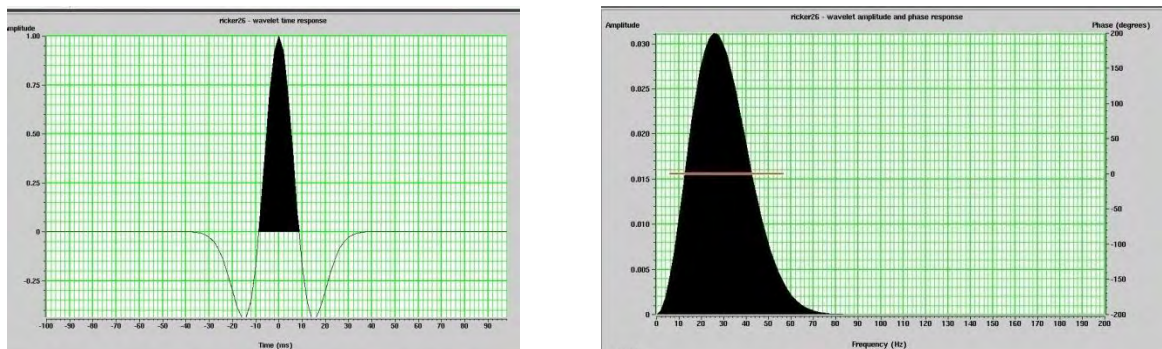


Figure 3.16 Left panel shows an extracted wavelet from full stack seismic. Right panel shows an amplitude spectrum in frequency domain.

Table 1 the calculation of tuning thickness and limit of detectability of two sands formations

Depths(m)	Thickness(m)	Frequency (Hz)	Velocity(m/s)	Tuning thickness(m)	Limit of detectability (m)
868-878	10	27.6	2516	22.8	9.1
1275-1280	5	26	2810	27	10.8
1280-1295	15	26	2650	25.4	10.2
1300-1335	35	26	2720	26.15	10.4
1345-1380	35	26	2694	25.9	10.3
1395-1430	65	26	3010	27.9	11.1

Form this study area, the thickness of reservoirs at the shallow depth is 10 meter which thinner than tuning thickness while the deep depth are around 31 meters which thicker than tuning thickness. So, we could identify top and bottom of reservoir only at the deep sand formation. Although, the deep sand formations have bed thicknesses greater than tuning thicknesses but shales as cap rocks that overlie sand are thinner than tuning thickness. So, we assumed that all sands at deep depth are appeared as one sand formation in order to analyze by AVO intercept-gradient analysis. Since, the model of acoustic impedance were available from the previous methods, these logs were used to create synthetic AVO gathers. Such modeling is performed to know whether an AVO response should be theoretically expected in any particular geological environment and target depth. Non-zero offset reflection coefficients are calculated using Aki-Richard equations while angles variation is calculated by ray-tracing through a velocity model derived from seismic velocities. A zero-phase ricker wavelet is extracted from the seismic data and then convolved with the reflection coefficients. Gradient analysis was performed to measure theoretical amplitude variation with angle for gas sand, oil sand and wet sand

A.

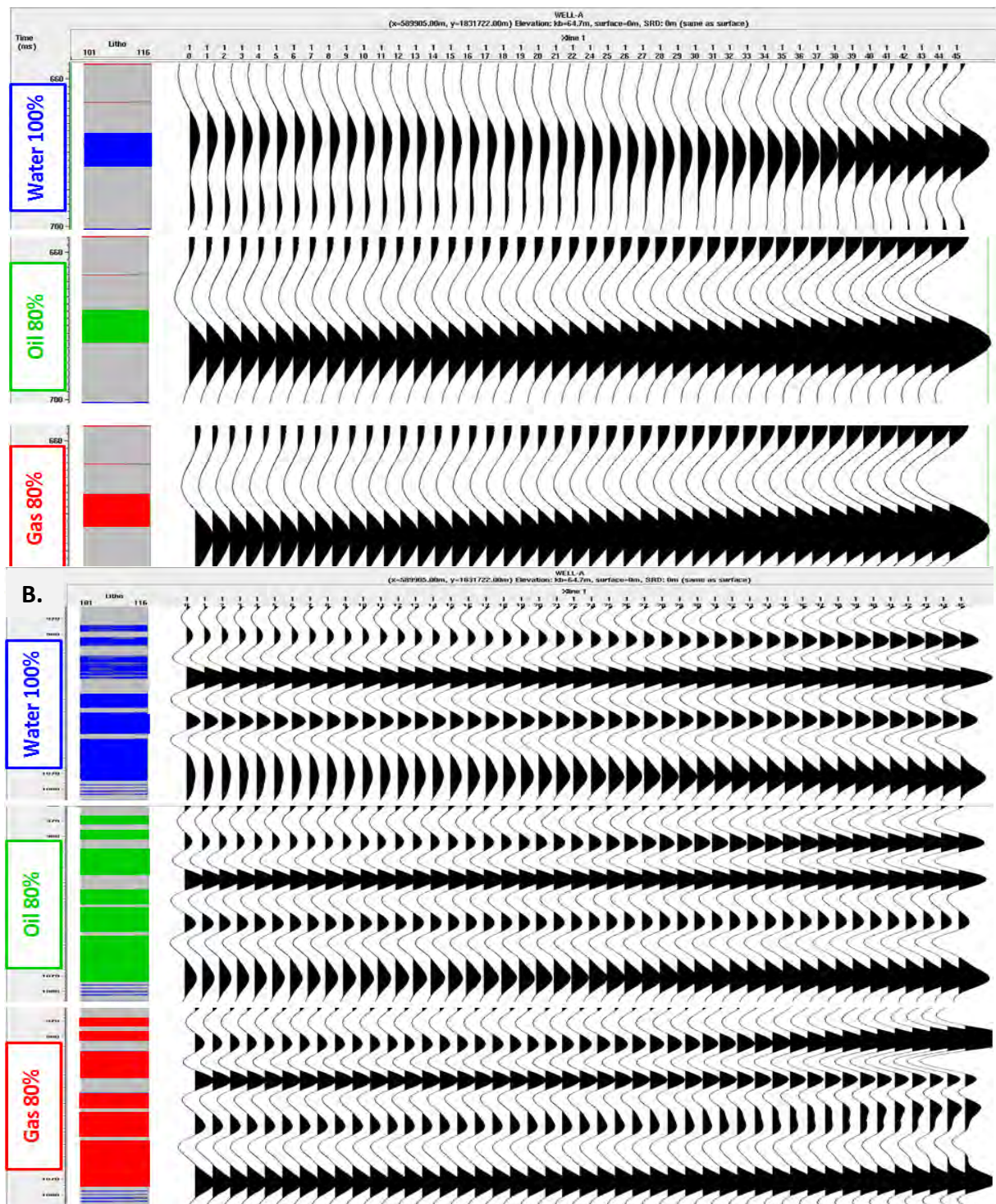


Figure 3.17 The shallow (A) and deep (B) sands formation of gas sands; oil sands and water sands represent the amplitude responses of top and bottom of sands. Because of shallow sands formation are thinner than tuning thickness so, amplitudes cannot divide top and bottom of sand formation but at the deep depth sands were thick thus, it's obviously divide top and bottom of these sands.

The results from AVO gradients show that the amplitude values change with offset (the distance between sources and receivers) by which the more offset also caused the more intercept angle and reflection coefficient that represent seismic amplitude. Reflection coefficient is the values that measured the difference of lithology properties.

The AVO curves and AVO cross plots of two sands formations represent AVO class 2 or class 3 which are similar to the result of depth tend analysis. In this study, we interested in top sand (assume that shales overlies sands) shown in red lines from the figures. Sands and shales at shallow and deep depth are near to tuning thickness. As the results, measurement of amplitude for wet sand, oil sand and gas sand showed decrease in amplitude with angle (Figure 3.17). These modeling helped give confidence that AVO might work for reservoirs greater than tuning thickness. Below tuning thickness and above the limit detectability AVO cannot be used to identify fluid types when the reservoir thickness is thinner than the limit of detectability; unfortunately this is the case for the majority of reservoirs in the study area. The top of water sand, oil sand and gas sand are also show negative reflection coefficient that classified as AVO class 2 or class 3 which the intercepts of amplitudes of water 100%, oil 80% and gas 80% increase respectively. The AVO gradients indicate that how seismic amplitude responses with increasing angles, the gradient of water 100%, oil 80% and gas 80% are more negative at high angles. And from the AVO cross-plots of all formations and fluid types, they are in quadrant 3 as AVO class2 or class 3.

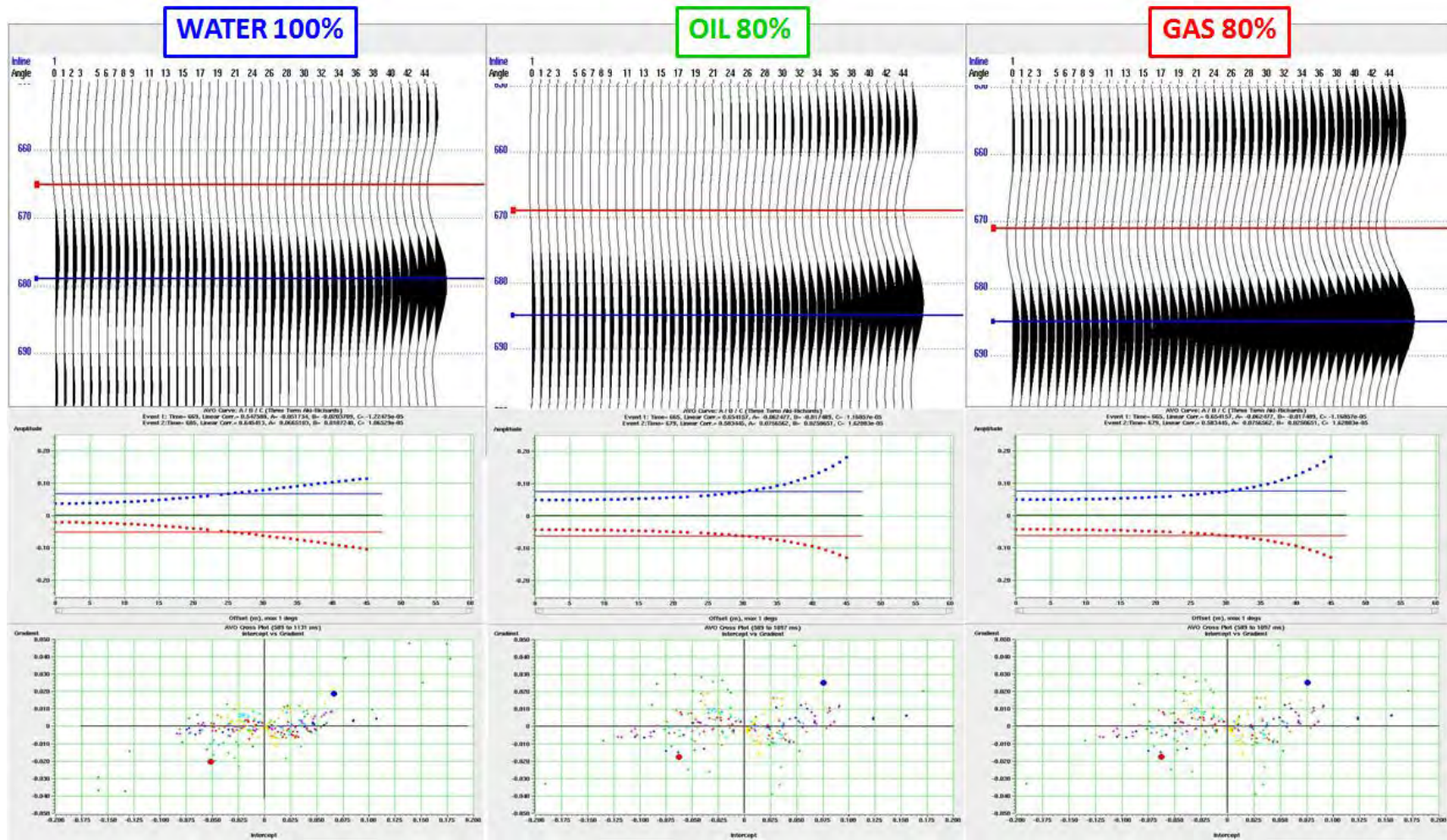


Figure 3.18 Measurement of amplitude with angle at shallow depth for top and base of wet sand, oil sand and gas sand, amplitude decrease with angle for the majority of the range

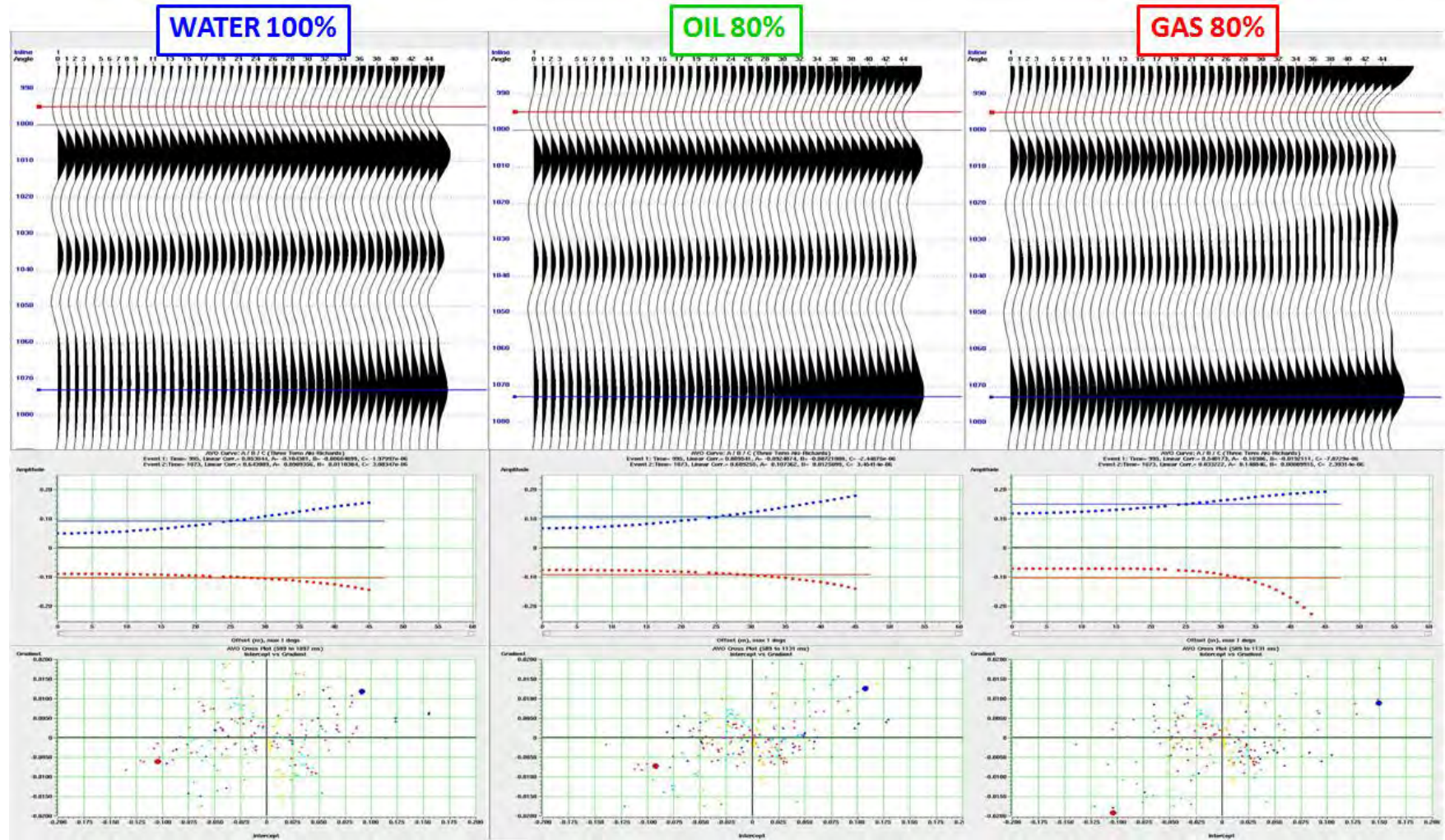


Figure 3.19 Measurement of amplitude with angle at deep depth for top and base of wet sand, oil sand and gas sand, amplitude decrease with angle for the majority of the range

CHAPTER 4: CONCLUSION AND DISCUSSION

In our study, we interested in two sand formations that are in 868-878 meters and 1282-1430 meters depth. The depth trends analysis of the modeled wet sands, oil sand and gas sand were observed to be either class 2 or class 3 according to Rutherford's AVO classification system if we considered an interface that shales overlies sands. AVO modeling showed that at shallow depth we can observe a measurable AVO response, while at deep depth most of shales were thinner than tuning thickness so we would not discriminate the top and bottom of that shale. Accordingly, AVO at the deeper depth could not be picked only one bed but have to pick as a group of shale beds in order to see their AVO responses. From AVO curves and cross plots, hydrocarbons sands give AVO intercept and gradient higher and lower than water sands. However when consider gas and oil sands there are slightly difference AVO responses between them in shallow formation. While at deep formation the intercept and gradient of water sands are similar to those of oil sands. Gas sands give highest intercept with significant decreasing amplitudes with angles. If the amplitudes of fluids are relatively similar, in seismic data we may not be able to distinguish between hydrocarbons and water sands. These may be caused by the amplitude effect decline as the bed thickness decrease below the tuning thickness.

REFERENCES

- Aki, K. and Richards, P.G., 1980. Quantitative Seismology. W.H. Freeman and Co.
- Casgatana, J., Swan, H., and Foster, D., 1998, Framework for AVO gradient and intercept interpretation: Geophysics, 63, 948-965.
- Gassmann, F., 1951, Elastic waves through a packing of spheres: Geophysics, 16, 673-685
- Han, D. and Batzle, M.L., 2004, Gassmann's equation and fluid-saturation effects on seismic velocities: Geophysics, 69, 398-405.
- Rutherford, S. and Williams, R., 1989, Amplitude-versus-offset variation in gas sands: Geophysics, 54, 680-688
- Simm, R., 2007, Practical Gassmann fluid substitution in sand/shale sequences: Geophysics, 25, 61-68
- Shuey, R., 1985, A simplification of Zoeppritz equations: Geophysics, 50, 609-614.
- Wang, Z., and Nur, A., 1992, Elastic wave velocity in porous media: A theoretical recipe. In Seismic and Acoustic Velocities in Reservoir Rocks, vol 2, SEG Geophysics Reprint series no.10
- Wang, Z., and Nur, A., 1989, Fundamental of seismic rock physics: Geophysics, 66, 308-41
- .